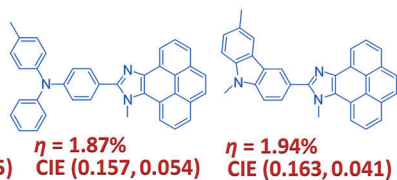
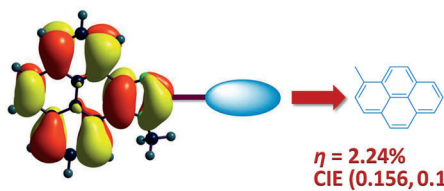


FULL PAPER



Deep-blue something: New pyrroloimidazoles showed blue emission with a high quantum efficiency and thermal stability and low oxidation potential.

The 10-pyrenyl pyrroloimidazole gave a driving voltage of 5.3 eV and a brightness of 2736 cd m^{-2} .

OLEDs

Dhirendra Kumar, K. R.
Justin Thomas,* Ching-Chiao Lin,
Jwo-Huei Jou*

Pyrroloimidazole-Based Deep-Blue-Emitting Materials: Optical, Electrochemical, and Electroluminescent Characteristics



Pyrenoimidazole-Based Deep-Blue-Emitting Materials: Optical, Electrochemical, and Electroluminescent Characteristics

Dhirendra Kumar,^[a] K. R. Justin Thomas,*^[a] Ching-Chiao Lin,^[b] and Jwo-Huei Jou*^[b]

Abstract: A series of pyrenoimidazoles that contained various functional chromophores, such as anthracene, pyrene, triphenylamine, carbazole, and fluorene, were synthesized and characterized by optical, electrochemical, and theoretical studies. The absorption spectra of the dyes are dominated by electronic transitions that arise from the pyrenoimidazole core and the additional chromophore. All of the dyes exhibited blue-light photoluminescence with moderate-to-high quantum efficiencies. They also displayed high thermal stability and their thermal-decom-

position temperatures fell within the range 462–512 °C; the highest decomposition temperature was recorded for a carbazole-containing dye. The oxidation propensity of the dyes increased on the introduction of electron-rich chromophores, such as triphenylamine or carbazole. The application of selected dyes that featured additional chro-

mophores such as pyrene, carbazole, and triphenylamine as blue-emissive dopants into multilayered organic light-emitting diodes with a 4,4'-bis(9H-carbazol-9-yl)biphenyl (CBP) host was investigated. Devices that were based on triphenylamine- and carbazole-containing dyes exhibited deep-blue emission (CIE 0.157, 0.054 and 0.163, 0.041), whereas a device that was based on a pyrene-containing dye showed a bright-blue emission (CIE 0.156, 0.135).

Keywords: density functional calculations • heterocycles • luminescence • organic light-emitting diodes • pyrenoimidazoles

Introduction

The development of suitable organic dyes for use in organic light-emitting diodes (OLEDs) has received immense attention owing to their applications in flexible, lightweight, and power-saving displays and illumination devices.^[1] Such dyes are often used as primary-color emitters,^[2] charge transporters,^[3] charge injectors,^[4] charge blockers,^[5] and even as hosts^[6] for singlet or triplet emitters in such devices. The development of new organic materials with multiple functional properties has been extensively explored for improving the device performance and minimizing the number of layers that are involved in the electroluminescent devices. For the commercialization of OLEDs, the development of stable and highly efficient three-primary-color (red, green, and blue) emitters is important.^[7] Deep-blue-light-emitting ma-

terials are of particular importance because of their applications as emitters^[8] and hosts for green- or red-phosphorescent materials^[9] if they possess suitable triplet energy levels. However, of the three basic colors that are required for full-color OLED devices, only a limited number of blue-light-emitting small molecules have been demonstrated to exhibit high efficiency, stability, and color purity.^[10] In view of such scarcity, there is much active research on blue-light-emitting chromophores. So far, the most-promising blue-light-emitting materials have been derived from polyaromatic hydrocarbons, such as fluorene^[11] and anthracene.^[12] Recently, pyrene-based^[13] molecular materials that possess other functional chromophores have also been developed and demonstrated as deep-blue-light emitters.

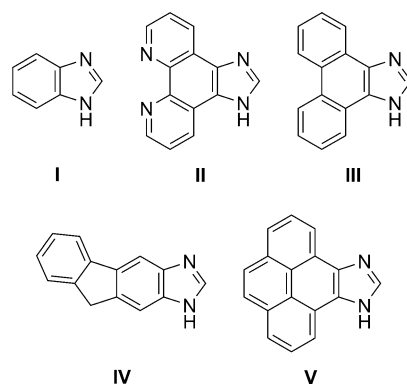
Pyrene contains an extensive π-conjugated system and displays high photoluminescence efficiency, enhanced thermal stability, and also promising carrier mobility.^[14] Because of its unique optical and electronic properties, pyrene has attracted much attention as an important scaffold in organic materials for application in OLEDs^[15] and organic field-effect transistors (OFETs),^[15b,16] as well as in photovoltaic devices, such as bulk heterojunction (BHJ) solar cells^[17] and dye-sensitized solar cells (DSSCs).^[18] The optical and electrochemical properties of pyrene derivatives can be easily tuned by incorporating electron-donors or acceptors and also by simply altering the chromophore loading through substitution at different positions.^[15b,19] Despite these advantages, pyrene suffers from its propensity to form π aggregates in the solid state, which significantly decreases its utili-

[a] D. Kumar, Dr. K. R. J. Thomas
Organic Materials Laboratory, Department of Chemistry
Indian Institute of Technology Roorkee
Roorkee 247 667 (India)
Fax: (+91)1332-286202
E-mail: krjt8fcy@iitr.ernet.in

[b] C.-C. Lin, Prof. J.-H. Jou
Department of Material Science and Engineering
National Tsing Hua University
Hsinchu 30013 (Taiwan)
E-mail: jjou@mx.nthu.edu.tw

 Supporting information for this article is available on the WWW under <http://dx.doi.org/10.1002/asia.201300271>.

ty in OLEDs.^[20] However, by making subtle structural variations, in particular through the introduction of sterically demanding groups, such as *tert*-butyl or diarylamine units, pyrene derivatives have been tuned to exhibit useful emission characteristics.^[21] Pyrene derivatives those have been exploited in efficient blue OLEDs include polypyrenes,^[21d,22] diphenylbenzene,^[23] alkynylpyrene,^[21c,24] pyrene-functionalized calix[4]arenes,^[25] and aryl-functionalized pyrenes,^[13a,21a,26] as well as pyrene–carbazole,^[24b,27] pyrene–fluorene,^[28] pyrene–triphenylamine,^[29] and pyrene–anthracene^[30] hybrids. In general, it has been observed that the hybridization of two functional units often leads to improvement in the device performance.^[27–30] With this result in mind, we have focused our attention on the less-explored pyrenoimidazole derivatives. Fused imidazoles (Scheme 1), such as benzimidazole (**I**),^[31] phenanthroline-imidazole (**II**),^[32] phenanthroimidazole (**III**),^[33] and fluorenoimidazole (**IV**),^[34] have been used in the construction of blue-light-emitting materials. Benzimidazole and phenanthroline-imidazole



Scheme 1. Benzimidazole (**I**), phenanthroline-imidazole (**II**), phenanthroimidazole (**III**), fluorenoimidazole (**IV**), and pyrenoimidazole (**V**).

Abstract in Hindi:

कार्यात्मक क्रोमोफोर्स जैसे एंश्रासीन, पाइरीन, ट्राईफेनीलएमीन, कार्बाज़ोल और फ्लूओरीन युक्त पाइरीनोइमिडाज़ोल्स का संश्लेषण एवम् प्रकाशीय, वैद्युत-रासायनिक और सैद्धांतिक अध्ययनों के द्वारा विश्लेषण किया गया। रंजकों के अवशोषण स्पेक्ट्रा पर पाइरीनोइमिडाज़ोल भाग एवं अतिरिक्त क्रोमोफोर से उत्पन्न होने वाले इलेक्ट्रॉनिक ट्रांजिसन्स का प्रभुत्व पाया गया। सभी रंजक मध्यम से उत्तम क्लांटम मात्रा के साथ नीली प्रकाशीय-चमक दर्शाएं। वे उच्च तापीय दृढ़ता भी प्रदर्शित किए और कार्बाज़ोल-युक्त रंजक के लिए उच्चतम अपघटन तापमान दर्ज करने के साथ उनके तापीय अपघटन तापमान 462–512 °C की सीमा में पाए गए। इलेक्ट्रान-संपन्न क्रोमोफोर्स जैसे ट्राईफेनीलएमीन अथवा कार्बाज़ोल को शामिल करने पर रंजकों की ऑक्सीकरण प्रवृत्ति में वृद्धि हुई। चयनित रंजक जिनमें पाइरीन, कार्बाज़ोल और ट्राईफेनीलएमीन जैसे अतिरिक्त क्रोमोफोर्स निहित थे, उनका अनुप्रयोग नीले डोपेंट्स के रूप में होस्ट 4,4'-विस(9H-कार्बाज़ोल-9-इल)वाईफिनाइल (सी.बी.पी.) के साथ बहु-स्तरित कार्बनिक प्रकाश-उत्सर्जक उपकरणों में विवेचन किया गया। कार्बाज़ोल और ट्राईफेनीलएमीन-युक्त रंजकों पर आधारित उपकरणों से गहरेनीले (CIE 0.159, 0.054 एवम् 0.163, 0.041), जबकि पाइरीन-युक्त रंजक पर आधारित उपकरण से उजले-नीले (CIE 0.156, 0.135) प्रकाश का उत्सर्जन हुआ।

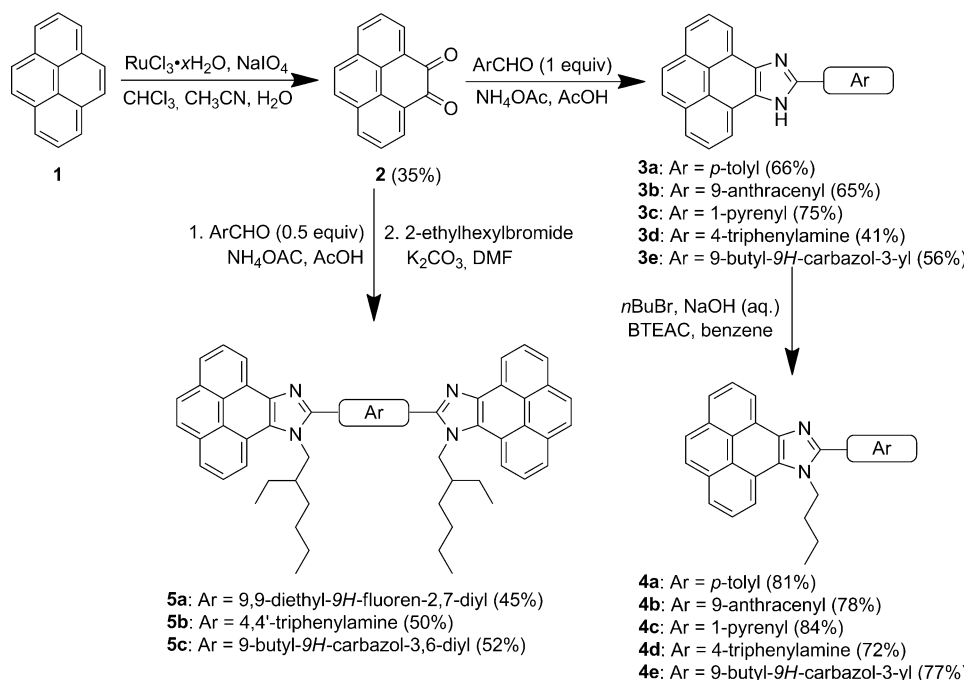
moieties has also been shown to be good electron-transporting materials^[32a,35] for OLEDs, owing to their strong electron affinity. In contrast, phenanthroimidazole^[33] and fluorenoimidazole^[34] derivatives have displayed low oxidation potentials and longer-wavelength photophysical characteristics compared to their corresponding benzimidazole analogues, owing to elongation of the conjugation in the former compounds. On this basis, we expected that the pyrenoimidazole moiety (**V**), with their outer π-electron cloud, would definitely enhance the electron density on the imidazole segment and the resulting materials might display unique electronic properties.^[36]

We have previously used the pyrenoimidazole moiety in the construction of organic dyes that possessed a donor–acceptor molecular configuration and demonstrated them to be promising sensitizers in dye-sensitized solar cells.^[37] Herein, we report eight new pyrenoimidazole-based luminescent materials and evaluate their photophysical, electrochemical, and electroluminescence characteristics. Time-dependent density functional theory (TDDFT) computations have also been performed to understand the electronic structure of these molecules. Molecular hybrids between pyrenoimidazole and fluorene, anthracene, pyrene, triphenylamine, and carbazole have been developed by using simple synthetic procedures. The optical properties of this class of compounds were affected by the nature of the chromophore that was attached onto the pyrenoimidazole moiety, thus revealing strong electronic coupling between the constituent units. Subsequently, emitters of deep-blue-to-cyan light have been realized and the deep-blue-light emitters have been found to effectively function as doped emitters in multilayered organic light-emitting diodes.

Results and Discussion

Synthesis and Characterization

The synthetic pathways that we employed to obtain the target compounds are shown in Scheme 2. The pyrene-4,5-dione was prepared by the oxidation of pyrene in the presence of ruthenium trichloride and sodium periodate.^[38] It



Scheme 2. Synthesis of pyrenoimidazole derivatives **4a–4e** and **5a–5c**.

was then reacted with the corresponding aldehyde in the presence of ammonium acetate to form the sparingly soluble imidazoles. Alkylation was either performed under phase-transfer catalysis conditions to afford mono-imidazoles (**4a–4e**) or by using $\text{K}_2\text{CO}_3/\text{DMF}$ to afford bis-imidazoles (**5a–5c**). Reasonably soluble products were obtained by introducing *n*-butyl groups into the mono-imidazoles or 2-ethylhexyl units into the bis-imidazoles. The compounds were thoroughly characterized by IR and NMR (^1H and ^{13}C) spectroscopy and by mass spectrometry. The analytical data were found to be consistent with the proposed structures.

Photophysical Properties

The photophysical properties of the dyes were investigated by absorption and fluorescence spectroscopy. The absorption and emission spectra of the compounds were recorded in various solvents, such as toluene, CH_2Cl_2 , CHCl_3 , DMF, MeCN, and MeOH, to study the effect of solvent polarity on their optical properties.

The absorption spectra of pyrenoimidazole derivatives in toluene are shown in Figure 1 and the pertinent data are compiled in Table 1. All of the compounds showed complex absorption profiles, owing to multiple localized $\pi\text{--}\pi^*$ transitions, which originated from the pyrenoimidazole segment and the chromophore that was tethered at the C10 position. The observed peak in the longer-wavelength region with vibrational fine structure is attributed to pyrenoimidazole-localized $\pi\text{--}\pi^*$ electronic excitation. This peak is significantly red-shifted compared to the analogous absorptions for the phenanthroimidazole and fluorenoimidazole analogues.^[33–34a] This result suggests the presence of more-extended con-

jugation in the pyrenoimidazole unit. The molar extinction coefficients of this transition followed the order: **4a** (*para*-tolyl) < **4b** (anthracene) < **4e** (carbazole) < **4c** (pyrene) < **4d** (triphenylamine) for the mono-imidazoles and **5c** (carbazole) < **5b** (triphenylamine) < **5a** (fluorene) for the bis-imidazoles. The bis-derivatives showed more than two-fold-higher molar extinction coefficients than the corresponding mono-derivatives at lower energies, thus indicating a doubled chromophore density and confirming the origin of absorption from the pyrenoimidazole unit.

The absorption spectra of the pyrenoimidazole derivatives are less sensitive towards the solvent polarity, which indicates

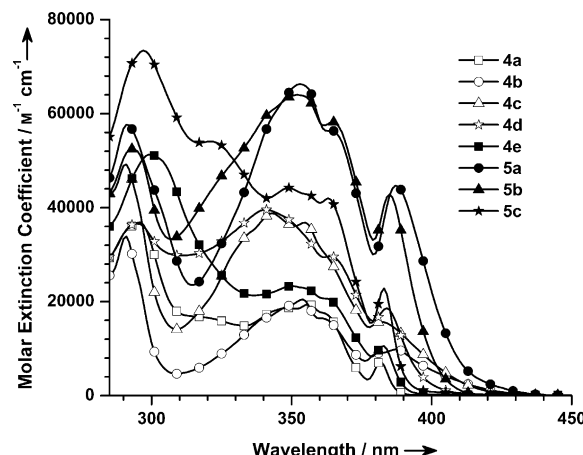


Figure 1. Absorption spectra of compounds **4a–4e** and **5a–5c** in toluene.

that the interaction of the dyes with the solvents in the ground state is less significant.

The emission spectra of the pyrenoimidazoles were measured in a series of solvents with different polarity. The emission spectra of the compounds in toluene are shown in Figure 2. In contrast to the absorption properties, the emission properties depend on the auxiliary chromophore that is present on the pyrenoimidazole segment. If the emission purely originates from the pyrenoimidazole-localized excited state, then the emission profile should be similar, irrespective of the chromophore that is present. Interestingly, the compounds that contained *para*-tolyl and carbazole moieties (**4a**, **4e**, and **5c**) exhibited similar emission profiles within the region 360–460 nm. This result suggests that the emis-

Table 1. Absorption properties of compounds **4a–4e** and **5a–5c** in different solvents.

Dye	λ_{abs} [nm] ($\epsilon \times 10^3$ [$\text{M}^{-1} \text{cm}^{-1}$])					
	Toluene	CH_2Cl_2	CHCl_3	DMF	MeCN	MeOH
4a	382 (7.2)	381 (6.5)	376 (6.2)	381 (7.8)	380 (6.6)	377 (5.6)
	356 (19.5)	353 (19.2)	357 (5.2)	353 (29.9)	349 (18.2)	345 (18.8)
	296 (36.9)	292 (39.2)	339 (29.6)	292 (40.2)	290 (38.6)	332 (16.3)
			324 (27.0)			314 (14.7)
			278 (36.3)			286 (38.2)
				278 (32.3)		
					286 (38.2)	
						278 (33.2)
4b	387 (9.8)	387 (10.5)	394 (8.2)	388 (10.6)	385 (11.0)	386 (9.7)
	354 (20.5)	351 (20.8)	375 (10.7)	381 (9.7)	360 (14.4)	376 (8.5)
	291 (33.9)	290 (34.7)	355 (8.3)	351 (21.2)	348 (20.6)	366 (10.1)
			338 (26.4)	290 (35.2)	288 (34.2)	345 (20.3)
			323 (17.6)			331 (15.2)
			309 (11.8)			285 (33.4)
				278 (33.2)		
					285 (33.4)	
4c	382 (15.7)	381 (14.9)	380 (15.2)	382 (16.4)	380 (14.5)	377 (13.6)
	355 (36.8)	344 (43.7)	341 (39.5)	344 (44.3)	342 (43.5)	342 (49.5)
	343 (38.8)	289 (50.7)	280 (51.0)	289 (52.1)	288 (50.0)	329 (38.4)
	291 (49.2)	279 (52.0)		279 (51.2)	277 (50.6)	285 (57.5)
						277 (56.4)
						277 (56.4)
4d	384 (18.6)	383 (17.1)	383 (31.1)	383 (19.0)	382 (16.8)	379 (16.1)
	364 (29.7)	339 (39.6)	345 (39.8)	363 (29.3)	336 (41.6)	335 (47.2)
	341 (39.5)	292 (36.7)	279 (33.9)	339 (41.7)	290 (39.9)	287 (44.1)
	295 (36.6)		269 (30.2)	292 (39.1)		
4e	383 (10.5)	381 (9.4)	379 (12.6)	382 (11.0)	381 (9.2)	378 (8.4)
	351 (23.3)	349 (22.4)	359 (14.1)	349 (23.6)	348 (21.8)	346 (25.3)
	299 (51.3)	298 (51.9)	340 (36.7)	298 (57.5)	297 (53.3)	334 (24.8)
			328 (34.0)		266 (36.2)	289 (58.6)
			280 (37.7)			268 (39.6)
5a	387 (44.7)	385 (43.0)	383 (38.3)	386 (45.1)	384 (42.8)	381 (40.2)
	364 (56.4)	350 (71.5)	340 (86.5)	364 (54.9)	362 (51.9)	360 (46.2)
	353 (66.3)	291 (63.1)	325 (59.2)	351 (69.9)	348 (70.7)	346 (77.5)
	291 (57.6)		310 (37.2)	291 (57.3)	289 (59.4)	285 (69.8)
			279 (72.6)			
5b	385 (42.8)	384 (37.7)	385 (47.3)	384 (38.5)	383 (38.3)	381 (36.2)
	365 (58.2)	363 (53.4)	364 (51.5)	364 (51.0)	362 (52.7)	360 (49.1)
	352 (64.0)	351 (62.0)	350 (56.7)	351 (59.0)	349 (64.4)	347 (67.6)
	293 (52.5)	292 (51.3)	280 (45.2)	292 (48.3)	289 (53.4)	286 (55.6)
5c	383 (22.8)	382 (19.6)	382 (24.0)	382 (21.8)	381 (19.4)	379 (18.5)
	363 (42.0)	361 (36.4)	343 (50.6)	362 (37.1)	360 (34.0)	359 (30.9)
	349 (44.2)	348 (40.5)	324 (50.7)	348 (41.4)	346 (41.0)	344 (46.4)
	321 (54.0)	295 (72.9)	293 (58.3)	296 (73.4)	293 (75.0)	312 (57.3)
	297 (73.4)		282 (58.3)			288 (79.8)

sion from these compounds mainly arises from the pyrenoidimidazole-localized electronic transition and the participation of the auxiliary chromophores in the transition is negligible. However, the dyes that possess triphenylamine (**4d**) and **5b**), fluorene (**5a**), pyrene (**4c**), and anthracene units (**4b**) exhibited red-shifted emission in that order. This result probably indicates the involvement of the auxiliary chromophores in the excited state of these compounds. It is likely that the excited state assumes a more-planar structure, thus giving room for the extension of conjugation to the auxiliary chromophore.^[39] A slight red-shift was observed for the bis-imidazole derivatives (**5b** and **5c**) when compared to their corresponding mono-imidazole analogues (**4d** and **4e**). This result further attests the partial involvement of auxiliary chromophores in the electronically excited state.

Among these dyes, the anthracene- (**4b**) and pyrene-containing dyes (**4c**) displayed pronounced Stokes shifts. This result could either be due to a significant structural reorientation in the excited state or to excimer formation. The fea-

tureless emission profiles (Figure 2) for these two dyes indicated the presence of strong inter-chromophoric electronic coupling in the excited state. In contrast, the *para*-tolyl (**4a**) and carbazole derivatives (**4e** and **5c**) exhibited very small Stokes shifts (204–336 cm⁻¹, Table 2).

With the exception of compounds **4a**, **4e**, and **5c**, all of these compounds showed positive solvatochromism, as shown for representative examples in Figure 3. The relatively poor sensitivity of compounds **4a**, **4e**, and **5c** towards the solvent environment (Table 2) may indicate a less-polar $\pi-\pi^*$ excited state that is localized within the pyrenoidimidazole unit. Although the peak positions of compounds **4a**, **4e**, and **5c** are not affected by the solvent polarity, the intensity ratio of the vibronic peaks undergo changes (Figure 3b) with the solvent polarity, analogous to those reported for polycyclic aromatic hydrocarbons, such as anthracene and pyrene.^[40] The solvent-dependent fluorescence of compounds **4b**, **4c**, **4d**, **5a**, and **5b** can be explained on the basis of general solvation effects with the Lippert–Mataga equation^[41] and the $E_T(30)$ parameter^[42] (Figure 4). The emission peak of these dyes shifted to longer wavelength on increasing the solvent polarity. This positive solvatochromism is indicative of a more-efficient solvation of the molecules in the excited state, that is, the stabilization of the excited state in polar solvents as compared to the ground state.^[43] The blue-shifted emission in MeOH may be ascribed to hydrogen-bonding interactions, which probably retard the reorientation of the fluorophore in the excited state by hindering the rotation of the aryl unit (Figure 5).^[44]

An abnormal red-shifted emission was observed in CHCl_3 for all of these compounds, which may be attributed to the involvement of carbene species that are generated upon the photoexcitation of

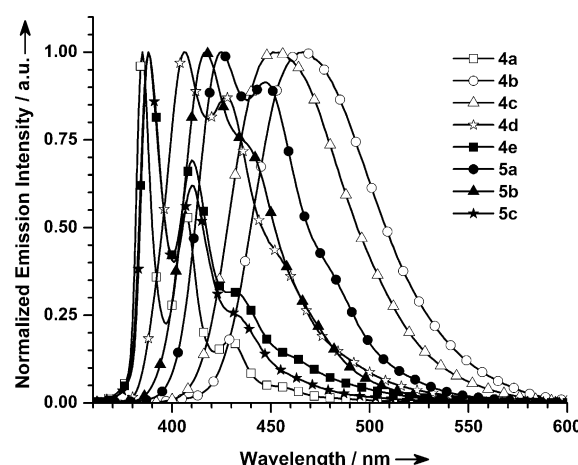


Figure 2. Emission spectra of compounds **4a–4e** and **5a–5c** in toluene.

Table 2. Emission properties and Stokes shift for compounds **4a–4e** and **5a–5c** in various solvents.

Dye	λ_{em} [nm] (Φ_F [%]) ^[a]				Stokes Shift [cm^{-1}]						
	Toluene	CH_2Cl_2	DMF	MeCN	MeOH	Film	Toluene	CH_2Cl_2	DMF	MeCN	MeOH
4a	385, 407, 430 (58)	384, 406, 428 (70)	384, 406, 428 (65)	383, 405, 427 (62)	380, 401, 424 (63)	464	204	205	205	206	209
4b	467 (62)	485 (34)	504 (26)	507 (22)	486 (28)	483	4427	5221	5932	6250	5331
4c	451 (97)	472 (84)	483 (76)	487 (73)	469 (75)	484	4005	5060	5474	5782	5203
4d	406, 427 (88)	429 (79)	445 (72)	449 (70)	435 (67)	494	1411	2834	3638	3906	3397
4e	388, 410, 428 (75)	388, 410 (81)	389, 412,	388, 404, 427 (78)	383, 410, 428 (74)	478	336	474	471	474	345
5a	425, 447 (99)	445 (98)	449 (94)	450 (92)	443 (94)	484	2310	3502	3635	3819	3673
5b	417 (87)	421 (90)	427 (88)	432 (84)	426 (82)	451	1993	2289	2622	2962	2773
5c	388, 410 (69)	388, 410 (67)	389, 411 (64)	387, 409 (61)	383, 405, 426 (60)	469	336	405	471	407	276

[a] Coumarin-1 ($\Phi_F=99\%$ in EtOAc) was used as a reference.

CHCl_3 . The effect of the acidic nature of halogenated solvents, such as CCl_4 and CHCl_3 , and their influence on the emission behavior of polyaromatic hydrocarbons are well-known in the literature.^[45] Notably, the electron-rich nature of the molecule dictated the outcome of such photochemical reactions. The deviations in the emission profile in CHCl_3 can be correlated with the π -accepting or π -donating ability of the aromatic unit that is linked to the pyrenoidimidazole nucleus. The compound that contains pyrene and anthracene units are not affected by CHCl_3 , whereas the other derivatives display shifts in accordance with their electron density, as identified from the oxidation potentials of the compounds (see above) of the units: fluorene (**5a**)<*para*-tolyl (**4a**)<carbazole (**4e** and **5c**)<triphenylamine (**4d** and **5b**; also see the Electrochemical Properties Section). The Stokes shift for derivatives **4a**, **4e**, and **5c** were less affected by the solvent polarity, which supported the rigidity of these molecules.^[46]

The emission spectra of the solid (drop-cast) films of pyrenoimidazole derivatives are shown in Figure 6. All of the

compounds showed featureless, broad, red-shifted emissions in films compared to those in toluene, which may be indicative of a close association of molecules in the solid state. Interestingly, the anthracene- (**4b**) and pyrene-containing derivatives (**4c**) showed a smaller shift, which was suggestive of their non-planar arrangement (see above), thus inhibiting an orderly arrangement in the solid state. The triphenylamine-containing mono-imidazole (**4d**) showed the most-red-shifted emission in the film compared to the corresponding bis-derivative (**5b**). The poor propensity for aggregation of the more-twisted bis-imidazole with a pyramidal triphenylamine segment is the reason for this observation. However, the carbazole-based mono- and bis-imidazoles exhibited similar shifts.

The photoluminescence quantum yields were determined by using coumarin-1 as a standard ($\Phi_F=99\%$ in EtOAc).^[47] All of the compounds showed very high quantum yields, in particular fluorene-, pyrene-, and triphenylamine-containing derivatives, which showed excellent fluorescence quantum yields (87–99 %) in solution. The high quantum yields for the triphenylamine derivatives overruled the presence of pronounced intramolecular charge transfer in these compounds, even in the excited state. However, a slight decrease in the quantum yield on moving from non-polar solvents to polar solvents suggest a weak dipole–dipole interaction between the molecules and the solvent.^[48]

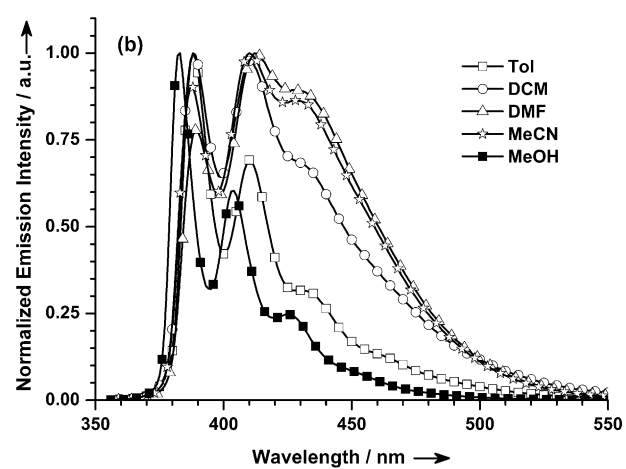
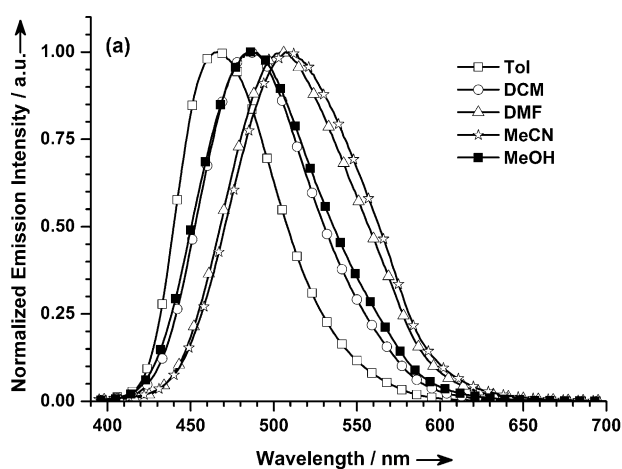


Figure 3. Emission spectra of compounds **4b** (a) and **4e** (b) in different solvents.

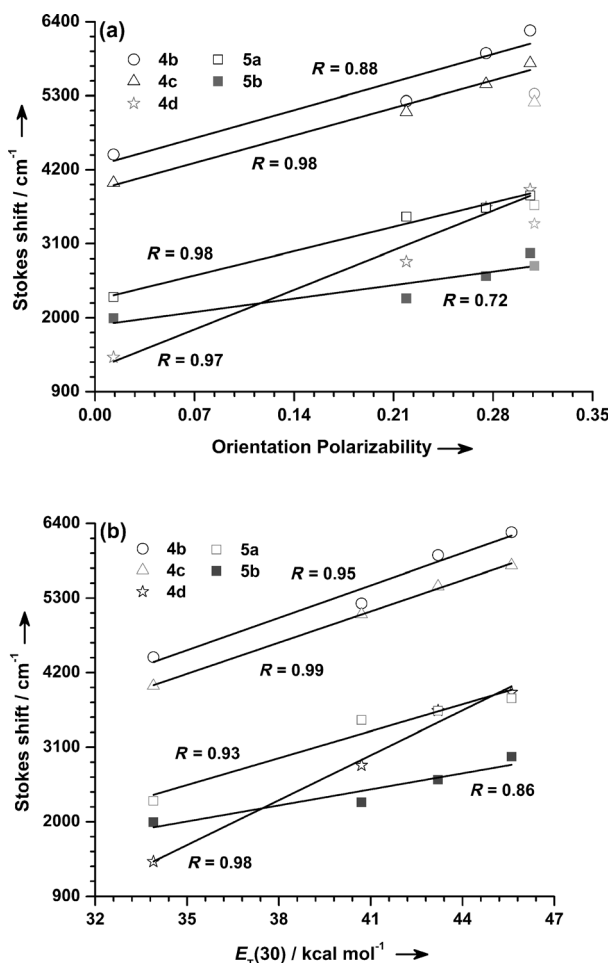


Figure 4. Correlation of the solvent-induced Stokes shift with a) orientation polarizability and b) the $E_T(30)$ parameter for compounds **4b**–**4d**, **5a**, and **5b**.

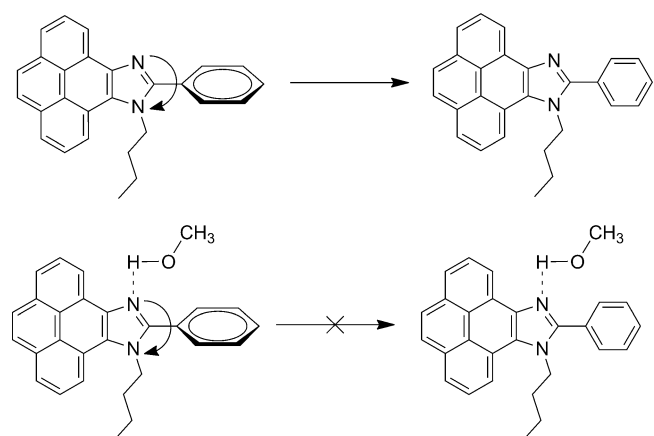


Figure 5. Hydrogen-bonding explanation for the observed blue-shifted emission in MeOH.

Electrochemical Properties

The electrochemical properties of these compounds were examined by using cyclic voltammetric (CV) and differential

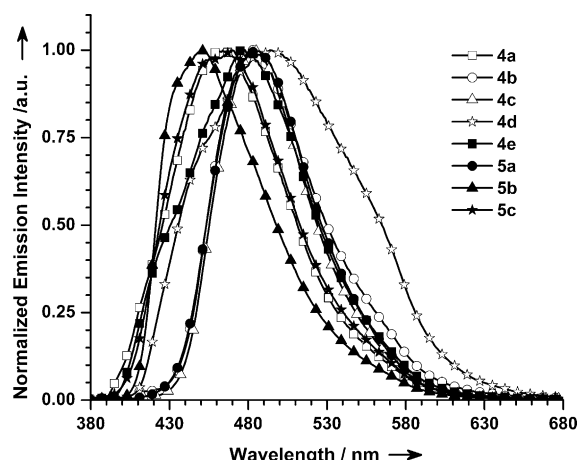


Figure 6. Emission spectra for the dyes as films.

pulse voltammetry (DPV). The redox potentials were calibrated by using the ferrocene/ferrocenium redox couple as an internal standard in each measurement. Selected data are collected in Table 3. All of the compounds exhibited irreversible peaks, which originated from the oxidation of pyrenoimidazole and/or auxiliary chromophores. Interestingly, the triphenylamine-based derivatives (**4d** and **5b**) showed a quasi-reversible redox couple in addition to the irreversible peak that was due to the removal of electron from the pyrenoimidazole moiety. The quasi-reversible oxidation process that occurred at high potential is attributed to the oxidation of the triphenylamine unit, in comparison to the value for the unsubstituted triphenylamine.^[49]

The first oxidation potentials for these compounds follow the order: **4b** (0.70 V) > **4c** (0.67 V), **4a** (0.65 V) > **4e** (0.56 V) > **4d** (0.50 V) for the mono-imidazoles and **5a** (0.68 V) > **5c** (0.55 V) > **5b** (0.53 V) for the bis-imidazoles. The more-electron-rich substituents facilitate the oxidation, as evidenced from the lower half-wave potentials for compounds **4d** and **5b**. Anthracene-containing derivative **4b** showed the highest oxidation potential because of its relatively enhanced π -accepting nature, whereas the electron-rich triphenylamine substituent caused the lowest oxidation potential in these series. The interplanar angle between the pyrenoimidazole and aromatic moieties also influenced the oxidative ability of the compounds, besides the electron density on the substituents, because it could alternate the electronic coupling between the two units. The dihedral angles (see above) in the imidazoles that contain aromatic substituents follow the trend: *para*-tolyl (**4a**) < pyrene (**4c**) < anthracene (**4b**), in accordance with their redox potentials. Presumably, a more-coplanar structure ensures the stabilization of the radical cation that is formed after oxidation of the imidazole unit. The lower oxidation potentials for these derivatives compared to the other reported fused imidazoles^[31d,32,33b] suggest the electron richness of the pyrenoimidazole moiety.

The HOMO energies of these compounds were calculated by using the ferrocene/ferrocenium redox couple as a refer-

Table 3. Thermal and electrochemical properties of compounds **4a–4e** and **5a–5c**.

Dye	T_d [°C] ^[a]	T_{onset} [°C] ^[b]	E_{ox} [V] ^[c] [mV])	ΔE_p [eV] ^[d]	HOMO [eV] ^[d]	LUMO [eV] ^[e]	E_{0-0} ^[f]
4a	462	356	0.65, 1.11	5.45	2.17	3.28	
4b	493	269	0.70, 1.08	5.50	2.53	2.97	
4c	500	447	0.67, 1.08	5.47	2.46	3.01	
4d	505	403	0.50, 0.72 (101), 1.05, 1.14	5.30	2.12	3.18	
4e	512	415	0.56, 1.04, 1.21	5.36	2.10	3.26	
5a	470	427	0.68, 1.08	5.48	2.40	3.08	
5b	464	430	0.53, 0.69 (91), 0.82, 1.02, 1.10	5.33	2.20	3.13	
5c	467	407	0.55, 1.07	5.35	2.09	3.26	

[a] Heating rate: 10 °C min⁻¹ under a nitrogen atmosphere. [b] Temperature that corresponds to a 5% weight loss. [c] Oxidation potentials with reference to the ferrocene/ferrocenium redox couple as an internal standard. [d] Determined from the equation HOMO = E_{ox} + 4.8. [e] Determined from the equation LUMO = HOMO - E_{0-0} . [f] Derived from the optical edge.

ence (4.8 eV)^[50] and were within the range 5.30–5.50 eV. The LUMO energies was calculated from their corresponding HOMO energies and the optical band gap as estimated from the intersection of the absorption and emission peaks, which ranged from 2.09 to 2.53 eV. The anthracene and pyrene derivatives showed low-lying LUMOs, in accordance with their π -accepting nature.^[27a,51]

Thermal Properties

The thermal properties of the pyrenoimidazole derivatives were investigated by using thermal gravimetric analysis; the pertinent data are presented in Table 3. All of the compounds showed very high thermal stability, as illustrated by their high thermal decomposition temperatures (T_d = 462–512 °C). The rigid pyrenoimidazole moiety is responsible for the high thermal stability. The substituents on the pyrenoimidazole nucleus also played an important role in determining the thermal stability of these compounds. Consequently, the thermal stability increased in the order: *para*-tolyl (**4a**) < anthracene (**4b**) < pyrene (**4c**) < triphenylamine (**4d**) < carbazole (**4e**) for the mono-imidazoles and fluorene (**5a**) < triphenylamine (**5b**) < carbazole (**5c**) for the bis-imidazoles. The bis-derivatives (**5b** and **5c**) possessed lower T_d values than their corresponding mono-derivatives (**4d** and **4e**), presumably owing to the presence of long alkyl chains in the former compounds. The carbazole-containing derivative (**4e**) showed remarkable thermal stability (T_d = 512 °C) in the series. Thermal stability of the carbazole derivatives is well-established in the literature.^[52]

Theoretical Calculations

To gain more insight into the photophysical behavior of these compounds, DFT calculations were performed for the pyrenoimidazole derivatives by using the Gaussian 09 program package.^[53] The lengthy alkyl chains were replaced by methyl groups in the model structures (**M4a–M4e** and

M5a–M5c; see the Supporting Information, Figure S57) to save computational time. We supposed that the replacement of the long alkyl chains by methyl groups would not affect the parameters that were relevant to this discussion. The unconstrained geometries of these compounds under vacuum were optimized by using DFT calculations with the Becke's three-parameter functional^[54] that was hybridized with the Lee–Yang–Parr correlation functional^[55] and the 6-31G(d,p) basis set.

The computed interplanar angles between the pyrenoimidazole and aromatic segments, the dipole moments, absorptions wavelengths, and oscillator strengths (*f*) for the most-appropriate transitions of the absorption bands of these compounds are reported in Table 4. The optimized geometries of these compounds showed that there was significant non-coplanarity between the pyrenoimidazole and C10-substituted segments. The anthracene-containing derivative showed a higher interplanar angle (about 69°) than the pyrene-containing derivative (about 49°). The other derivatives were moderately twisted from the plane of the imidazole unit (35–37°). The HOMOs of these compounds were generally localized over the entire molecule (Figure 7), whilst the LUMOs were generally spread over the different parts of the molecules. The π -aromatic segments, such as anthracene, pyrene, and fluorene, exclusively participated in constructing the LUMOs in compounds **4b**, **4c**, and **5a**. However, for the derivatives that contained *para*-tolyl, car-

Table 4. Computed interplanar angle, dipole moment, absorptions, and oscillator strengths (TDDFT/B3LYP/6-31G(d,p)) of structures **M4a–M4e** and **M5a–M5c**.

Dye	Angle [°] ^[a]	μ_g [Debye]	λ_{abs} [nm]	<i>f</i>	Assignment (%)
M4a	36.64	3.47	356.2	0.2306	HOMO→LUMO (90)
M4b	68.51	3.33	455.3,	0.0706,	HOMO→LUMO (99)
			387.4,	0.1224,	HOMO→1→LUMO (97)
			352.3	0.1197	HOMO→LUMO+1 (84)
M4c	48.77	3.08	425.7,	0.3429,	HOMO→LUMO (97)
			362.2	0.2381	HOMO→LUMO+1 (65)
					HOMO→1→LUMO (23)
M4d	34.95	3.56	378.8,	0.4937,	HOMO→LUMO (89)
			362.3	0.4401	HOMO→LUMO+1 (85)
					HOMO→2→LUMO (5)
M4e	36.21	4.16	364.6,	0.1778,	HOMO→LUMO (90)
			350.3	0.1435	HOMO→LUMO+1 (62)
					HOMO→LUMO+2 (24)
M5a	34.39	1.06	413.9,	1.2883,	HOMO→LUMO (96)
	37.30		359.2	0.1433	HOMO→LUMO+2 (78)
M5b	35.39	6.77	394.9,	1.2905,	HOMO→LUMO (77)
	35.40		351.7	0.2769	HOMO→LUMO+2 (17)
					HOMO→LUMO+3 (52)
					HOMO→1→LUMO (28)
					HOMO→1→LUMO+2 (8)
M5c	36.49	1.41	369.2,	0.2087,	HOMO→LUMO (87)
	36.54		354.4	0.1654	HOMO→LUMO+3 (6)
					HOMO→1→LUMO (93)

[a] Interplanar angle between the pyrenoimidazole moiety and the substituent at the C10 position.

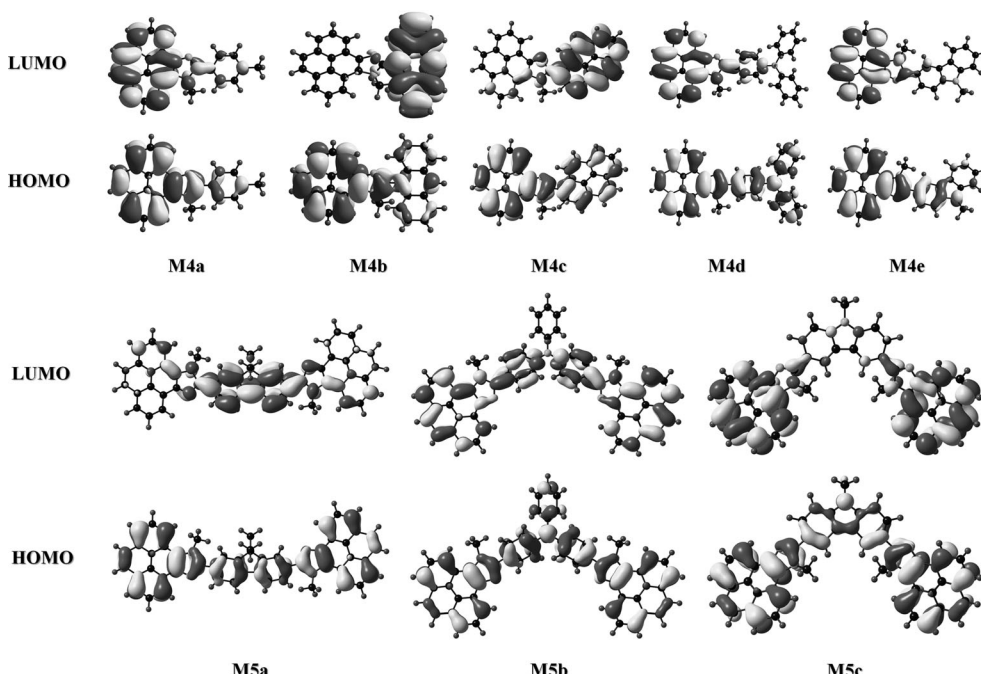


Figure 7. Frontier molecular orbitals (HOMOs and LUMOs) of structures **M4a**–**M4e** (top) and **M5a**–**M5c** (bottom).

bazole, and triphenylamine units, the LUMOs were mainly localized on the pyrenoimidazole unit. The trend in the experimentally observed longer-wavelength absorptions for these compounds matched well with the theoretical computed low-energy excitations.

The adiabatic and vertical ionization potentials for the compounds were also computed (Table 5) to gain insight into their charge-transport properties. The computed ionization potentials followed the order: **4a** > **4b** > **4c** > **4e** > **4d** for the mono-imidazoles and **5a** > **5c** > **5b** for the bis-imidazoles.

Table 5. Computed ionization potentials and electron affinities for structures **M4a**–**M4e** and **M5a**–**M5c**.

Dye	Adiabatic I_p [eV]	Vertical I_p [eV]	Adiabatic E_a [eV]	Vertical E_a [eV]
M4a	-6.256	-6.342	0.086	-0.045
M4b	-6.155	-6.258	0.683	0.560
M4c	-6.071	-6.155	0.660	0.542
M4d	-5.810	-5.912	0.250	0.083
M4e	-5.976	-6.079	0.064	-0.015
M5a	-5.803	-5.856	0.783	0.675
M5b	-5.631	-5.694	0.558	0.486
M5c	-5.796	-5.841	0.454	0.396

zoles. This trend matched that observed for the experimentally determined HOMO levels. In general, the presence of electron-rich groups, such as triarylamines and carbazole groups, or the elongation of conjugation in the molecule decreased the ionization energy. Triphenylamine-containing derivatives **4d** and **5b** showed the lowest I_p values, owing to the relatively high electron-donating nature of this group. The molecules with lower ionization potentials are expected to possess good hole-transporting capability. The adiabatic and vertical electron affinities (EA) of these compounds

were also calculated. The EAs of these compounds followed the trend: **4e** < **4a** < **4d** < **4c** < **4b** for the mono-imidazoles and **5c** < **5b** < **5a** for the bis-imidazoles, in good agreement with the experimentally determined LUMO energy values.

Electroluminescence Properties

The use of dyes **4c**, **5b**, and **5c** in multilayered OLED devices was also evaluated. These dyes were either simply applied as emitting materials, ITO/PEDOT:PSS/**4c** or **5b** or **5c**/TPBI/LiF/Al (device I), or as emitting dopants in a CBP host, ITO/PEDOT:PSS/CBP+**4c** or **5b** or **5c** (3, 6, or 9 wt. % each)/TPBI/LiF/Al (devices II–IV). The alignment of the energy levels in the materials that were used for the

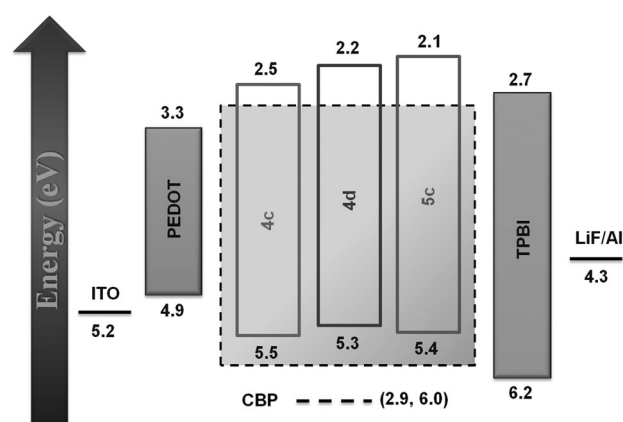


Figure 8. Energy-level diagram of the materials that were used for the fabrication of devices.

fabrication of these devices is shown in Figure 8. Figure 9 shows the current-density–voltage (I – V) and luminance–current-density (L – I) plots of the OLEDs that were fabricated by using these dyes as emitting dopants. The device-performance and electroluminescence (EL) emission characteristics are listed in Table 6. The devices with these dyes as neat emitters exhibit lower turn-on voltages when compared to the devices with these dyes as emitting dopants. This result is probably due to the larger hole-blocking barrier (1.1 eV)

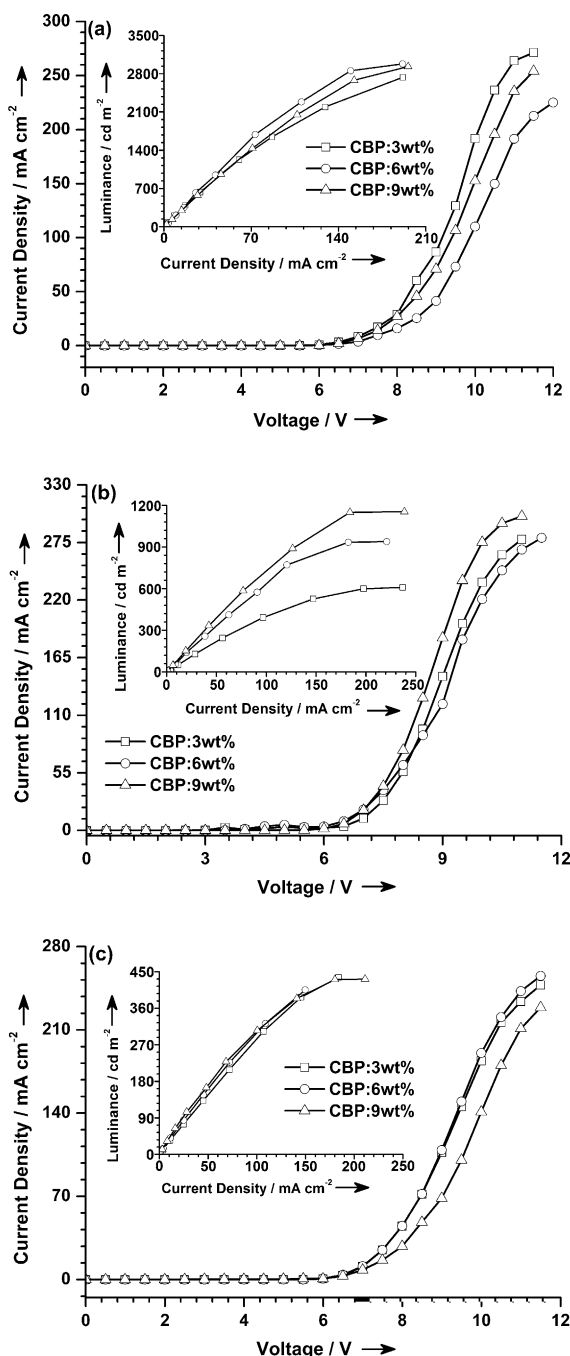


Figure 9. Current-density–voltage (I – V) and luminance–current-density (L – I) curves (inset) for devices that were doped with compounds **4c** (a), **5b** (b), and **5c** (c).

for the doped devices when compared to the neat devices (0.4–0.6 eV).

The EL spectra of the devices that incorporated these dyes as either neat films or as dopants at different concentrations are shown in Figure 10. The neat-film-based devices showed a red-shifted EL, similar to the photoluminescence (PL) observed for the film, which further confirmed the involvement of aggregation in the solid state. The devices with 3 wt. % dyes (device II) showed the most-blue-shifted EL, which was almost unaffected on increasing the concentration of the dye up to 9 wt. %. However the brightness varied in the cases of dyes **4c** and **5b**: Maximum brightness was observed for the devices that were doped with 6 wt. % of compound **4c** (2980 cd m^{-2}) and with 9 wt. % of compound **5b** (1154 cd m^{-2}). The device that was doped with compound **4c** showed bright-blue EL, whereas deep-blue EL was observed for the devices that were doped with compounds **5b** and **5c**. The highest brightness, which was obtained for the compound-**4c**-based devices, may be attributed to the balanced confinement of holes and electrons within the emitting layer, owing to the favorable hole- and electron-injection barriers at the HTL/EML and EML/ETL interfaces.

The efficiencies of the neat devices and the OLEDs that contained higher concentrations (6–9 wt. %) of the dyes were inferior to those of the devices that contained 3 wt. % of the dyes in the CBP host. Among these devices, the best performance was achieved for the device that employed compound **4c** (3 wt. %) as an emitting dopant (driving voltage: 5.3 eV; $\eta_{\text{ext}} = 2.24\%$; $\eta_c = 2.4 \text{ cd A}^{-1}$; $\eta_p = 1.2 \text{ Lm W}^{-1}$; CIE (0.156, 0.135); brightness: 2736 cd m^{-2}). In general, the performance of the doped devices (devices II–IV) were superior to those of the neat-film-based devices (device I), which may be attributed to aggregation of the dyes in the pure film, owing to their planar structural features. In addition, the efficient capturing of energy by the dyes from the CBP excitons is responsible for the better performance of the doped devices. The EL did not fluctuate with the variation in the cell voltage, which is beneficial for applications in commercial full-color displays.

Conclusions

A series of pyrenoimidazole-based luminescent materials have been synthesized and characterized. Pyrenoimidazoles that contained different chromophores exhibited blue luminescence with excellent photoluminescence quantum efficiency. The *para*-tolyl- and carbazole-containing derivatives showed featured emission with very low Stokes shifts in most of the solvents tested, thus revealing their rigid structure. Moreover, all of the compounds studied herein showed high thermal stability and lower oxidation potentials, which strengthened their eligibility in electroluminescent and hole-transporting materials for organic light-emitting devices. Solution-processed OLED devices based on compounds **4c**, **5b**, and **5c** as a dopant were successfully fabricated and showed decent device parameters. Devices based on com-

Table 6. Performance characteristics of devices based on compounds **4c**, **5b**, and **5c**.

Material	Conc. [wt. %]	Driving voltage [V]	Power ef- ficiency [Lm W ⁻¹]	Current efficiency [cd A ⁻¹]	External quantum ef- ficiency [%] @ 100/1000 cd m ⁻²	CIE coordinates	Max. lumi- nance [cd m ⁻²]
4c	neat	3.7	0.9/0.8	1.2/1.5	0.55/0.69	(0.196, 0.345)/(0.188, 0.330)	2510
4c+CBP	3	5.3	1.2/0.8	2.4/2.1	2.24/2.12	(0.156, 0.135)/(0.156, 0.126)	2736
	6	5.7	0.9/0.8	1.9/2.3	1.60/2.06	(0.155, 0.145)/(0.154, 0.137)	2980
	9	5.6	1.0/0.8	2.0/2.1	1.58/1.75	(0.156, 0.153)/(0.155, 0.145)	2931
	neat	3.6	0.7/0.5	0.9/0.9	0.71/0.76	(0.176, 0.176)/(0.170, 0.160)	1227
5b+CBP	3	5.9	0.2/-	0.4/-	1.53/-	(0.158, 0.045)/-	609
	6	5.5	0.3/-	0.7/-	1.86/-	(0.157, 0.049)/-	939
	9	5.5	0.4/0.3	0.8/0.7	1.87/1.56	(0.157, 0.054)/(0.157, 0.057)	1154
5c	neat	3.7	0.5	0.7	0.47	(0.185, 0.232)	736
5c+CBP	3	5.9	0.1	0.3	1.94	(0.163, 0.041)	436
	6	5.8	0.1	0.3	1.72	(0.163, 0.045)	435
	9	5.9	0.2	0.4	1.30	(0.163, 0.061)	432

pounds **5b** (CIE 0.157, 0.054) and **5c** (CIE 0.163, 0.041) exhibited deep-blue-light emission and bright-blue-light emission was observed for the device that was doped with compound **4c** (CIE 0.156, 0.135). The 3 wt. % compound-**4c**-doped device showed the best performance, with a driving voltage of 5.3 eV and a brightness of 2736 cd m⁻², with an external efficiency, current efficiency, and power efficiency of 2.24%, 2.4 cd A⁻¹, and 1.2 Lm W⁻¹, respectively.

Experimental Section

Material and Methods

Chemicals were purchased from Aldrich, SD Fine Chem, Spectrochem, or Thomas Baker and used as received. Solvents were dried and distilled immediately prior to use by using standard procedures. Purification by column chromatography was performed on silica gel (230–400 mesh, Rankem) as the stationary phase (column dimensions: 40 cm × 3.0 cm). ¹H NMR and ¹³C NMR spectra were recorded in CDCl₃ or [D₆]DMSO on a Bruker AV 500 O FT NMR spectrometer at 500.13 and 125.77 MHz, respectively. High-resolution mass spectrometry was performed on an ESI mass spectrometer. UV/Vis spectra were recorded at RT in quartz cuvettes on a UV-1800 Shimadzu spectrophotometer. Fluorescence measurements were performed on a RF-5301-PC Shimadzu spectrofluorophotometer. The quantum yield of the dyes were calculated by following a standard procedure and using coumarin-1 ($\Phi_F=0.99$ in EtOAc)^[47] as a reference. Corrections owing to dye absorption and refractive indices of the solvents were incorporated into the calculations. Cyclic voltammetry (CV) and differential pulse voltammetry (DPV) measurements were performed on a CHI 620C electrochemical analyzer in THF with 0.1 M tetrabutylammonium perchlorate as a supporting electrolyte. The experiments were performed at RT under a nitrogen atmosphere in a three-electrode cell that consisted of a Pt wire as an auxiliary electrode, a non-aqueous Ag/AgNO₃ reference electrode, and a glassy carbon working electrode. The HOMO energy levels of the organic materials were measured from the oxidation potentials, as obtained by cyclic voltammetry, and the LUMO energy levels were determined from the HOMO energy levels and the optical band gaps, as estimated from the intersection of the absorption and emission bands. Thermogravimetric analysis/differential thermal analysis/differential thermogravimetry (TGA-DTA-DTG) measurements were performed on a Perkin-Elmer Pyris Diamond at a heating rate of 10 °C min⁻¹ under a flow of nitrogen. All of the calculations for the geometrical and electronic properties of the dyes were performed in the gas phase by using the Gaussian 09 program package.

OLED Device Fabrication

The OLED devices were fabricated on a pre-cleaned glass substrate and were composed of a layer of indium tin oxide (thickness: 125 nm) as an anode, poly(3,4-ethylene-dioxythiophene)-poly(styrenesulfonate) (PEDOT:PSS, thickness: 35 nm) as a hole-injection layer (HIL), an emissive layer (EML), TPBI as an electron-transport layer, a LiF electron-injection layer (EIL, thickness: 0.7 nm), and an Al layer (thickness: 150 nm) as a cathode. The aqueous solution of PEDOT:PSS was spin-coated at 4000 rpm for 20 s to form the HIL layer (thickness: 35 nm). The dyes (**4c**, **5b**, and **5c**), either neat or doped into 4,4'-bis(9H-carbazol-9-yl)biphenyl (CBP), were deposited by spin-coating at 2500 rpm for 20 s; then, the TPBI layer was deposited onto it.

Subsequently, lithium fluoride and the aluminum cathode were thermally evaporated at a pressure of 1.0 × 10⁻⁵ Torr.

Synthesis

Pyrene-4,5-dione (**2**),^[38] 4-(diphenylamino)benzaldehyde,^[56] 4,4'-(phenylazanediyl)dibenzaldehyde,^[56] 9-butyl-9H-carbazole-3-carbaldehyde,^[56] and 9-butyl-9H-carbazole-3,6-dicarbaldehyde^[57] were synthesized according to literature procedures.

General Procedure for the Synthesis of 10-Aryl-9H-pyreno[4,5-d]imidazole (**3a–3e**)

Pyrene-4,5-dione (348 mg, 1.5 mmol), the corresponding aryl aldehyde (1.5 mmol), and ammonium acetate (578 mg, 7.5 mmol) were dissolved in acetic acid (10 mL) and the resultant mixture was heated at reflux for 24 h. Next, the reaction mixture was cooled and poured into water to obtain a precipitate, which was dried and washed with hot CHCl₃ to obtain the title compounds with sufficient purity for their direct use in further reactions.

10-*para*-Tolyl-9H-pyreno[4,5-d]imidazole (**3a**)

Pale-yellow solid; 66% yield; M.p. 220–222 °C; ¹H NMR ([D₆]DMSO, 500.13 MHz): δ = 13.66 (s, 1 H), 8.81–8.86 (m, 2 H), 8.29 (d, *J* = 8.5 Hz, 2 H), 8.24 (dd, *J* = 8.0 Hz, 1.5 Hz, 2 H), 8.12–8.19 (m, 4 H), 4.43 (d, *J* = 8.0 Hz, 2 H), 2.41 ppm (s, 3 H); ¹³C NMR ([D₆]DMSO, 125.77 MHz): δ = 150.1, 139.5, 138.0, 132.1, 131.9, 130.0, 128.5, 128.3, 128.2, 127.9, 126.8, 126.7, 126.6, 124.6, 124.5, 122.3, 122.2, 122.1, 119.5, 119.4, 21.5 ppm; HRMS (ESI): *m/z* calcd for C₂₄H₁₇N₂: 333.1386 [M+H]; found: 333.1395.

10-(Anthracen-9-yl)-9H-pyreno[4,5-d]imidazole (**3b**)

Yellow solid; 65% yield; M.p. 278–280 °C; ¹H NMR ([D₆]DMSO, 500.13 MHz): δ = 14.16 (s, 1 H), 8.92 (s, 1 H), 8.86 (d, *J* = 7.5 Hz, 1 H), 8.65 (d, *J* = 7.5 Hz, 1 H), 8.25–8.30 (m, 6 H), 8.15 (quin, *J* = 7.5 Hz, 2 H), 7.87 (d, *J* = 8.5 Hz, 2 H), 7.62 (t, *J* = 7.5 Hz, 2 H), 7.55 ppm (t, *J* = 7.5 Hz, 2 H); ¹³C NMR ([D₆]DMSO, 125.77 MHz): δ = 147.2, 137.4, 131.6, 131.5, 131.0, 130.8, 128.9, 128.6, 128.0, 127.97, 127.5, 127.0, 126.5, 126.3, 125.9, 125.7, 124.3, 124.1, 121.84, 121.80, 121.7, 119.2, 118.7 ppm; HRMS (ESI): *m/z* calcd for C₃₁H₁₉N₂: 419.1543 [M+H]; found: 419.1552.

10-(Pyren-1-yl)-9H-pyreno[4,5-d]imidazole (**3c**)

Yellow solid; 75% yield; M.p. 258–260 °C; ¹H NMR ([D₆]DMSO, 500.13 MHz): δ = 14.09 (s, 1 H), 9.68 (d, *J* = 7.5 Hz, 1 H), 8.99 (d, *J* = 7.5 Hz, 1 H), 8.91 (d, *J* = 7.0 Hz, 1 H), 8.77 (d, *J* = 8.0 Hz, 1 H), 8.56 (d, *J* = 8.0 Hz, 1 H), 8.40–8.43 (m, 3 H), 8.30–8.33 (m, 4 H), 8.17–8.25 ppm (m, 5 H); ¹³C NMR ([D₆]DMSO, 125.77 MHz): δ = 149.8, 149.6, 131.5, 131.4, 130.9, 130.4, 128.8, 128.6, 128.5, 128.3, 127.4, 127.3, 127.2, 126.6, 126.3, 125.8, 125.7, 125.5, 125.3, 125.0, 124.9, 124.8, 124.4, 124.3, 123.8, 121.9,

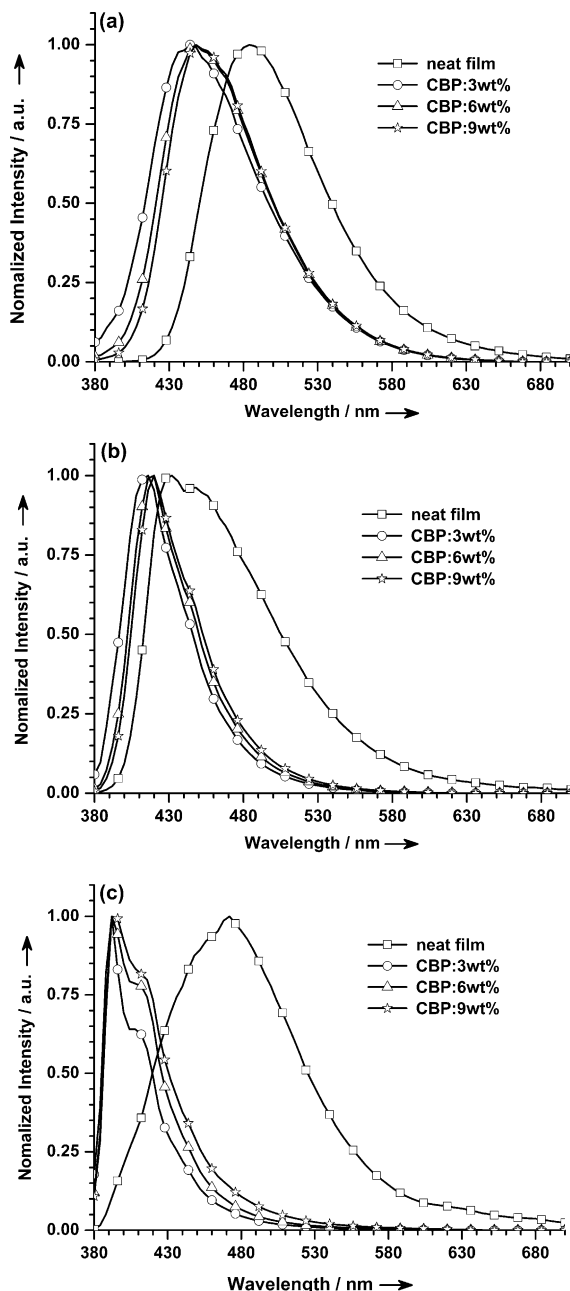


Figure 10. Electroluminescence spectra for the devices (I–IV) that were fabricated from compounds **4c** (a), **5b** (b), and **5c** (c).

121.7, 119.4, 119.2, 119.0 ppm; HRMS (ESI): m/z calcd for $C_{33}H_{19}N_2$: 443.1543 [$M+H$]; found: 443.1548.

*N,N-Diphenyl-4-(9H-pyreno[4,5-d]imidazol-10-yl)aniline (**3d**)*

Light-yellow solid; 41% yield; M.p. 285–287°C; ^1H NMR ([D_6]DMSO, 500.13 MHz): δ = 13.59 (s, 1H), 8.80 (s, 2H), 8.23–8.27 (m, 4H), 8.20 (s, 2H), 8.14 (t, J = 7.5 Hz, 2H), 7.36–7.40 (m, 4H), 7.16–7.18 (m, 2H), 7.12–7.15 ppm (m, 6H); ^{13}C NMR ([D_6]DMSO, 125.77 MHz): δ = 149.5, 148.3, 146.7, 137.5, 131.5, 131.4, 129.7, 128.0, 127.9, 127.5, 126.3, 126.2, 126.0, 124.7, 124.0, 123.8, 122.1, 121.6, 119.1, 118.8 ppm; HRMS (ESI): m/z calcd for $C_{35}H_{24}N_2$: 486.1965 [$M+H$]; found: 486.1974.

*10-(9-Butyl-9H-carbazol-3-yl)-9H-pyreno[4,5-d]imidazole (**3e**)*

White solid; 56% yield; M.p. > 300°C; ^1H NMR ([D_6]DMSO, 500.13 MHz) 9.27 (s, 1H), 8.95 (d, J = 7.5 Hz, 2H), 8.59 (dd, J = 8.5 Hz, 1.5 Hz, 1H), 8.32–8.35 (m, 1H), 8.20–8.23 (m, 4H), 8.14 (t, J = 7.5 Hz, 2H), 7.81 (d, J = 8.5 Hz, 1H), 7.67 (d, J = 8.0 Hz, 1H), 7.52 (dt, J = 7.5 Hz, 1 Hz, 1H), 7.29 (t, J = 7.5 Hz, 1H), 4.48 (t, J = 7.5 Hz, 2H), 1.83 (quin, J = 7.5 Hz, 2H), 1.37 (sext, J = 7.5 Hz, 2H), 0.92 ppm (t, J = 7.5 Hz, 3H); ^{13}C NMR ([D_6]DMSO, 125.77 MHz): δ = 151.2, 140.58, 140.56, 131.5, 127.6, 126.3, 124.6, 123.8, 122.3, 122.1, 121.6, 121.4, 120.5, 119.3, 119.0, 118.5, 109.71, 109.66, 42.2, 30.7, 19.8, 13.7 ppm; HRMS (ESI): m/z calcd for $C_{33}H_{26}N_3$: 464.2121 [$M+H$]; found: 464.2128.

*General Procedure for the Synthesis of 10-Aryl-9-butyl-9H-pyreno[4,5-d]imidazole (**4a–4e**)*

A mixture of 10-aryl-9H-pyreno[4,5-d]imidazole (1 mmol), 1-bromobutane (0.21 g, 1.5 mmol), benzyltriethylammonium chloride (BTEAC 0.10 g), a 50% aqueous solution of NaOH (10 mL), and benzene (5 mL) was heated at reflux for 6 h. After a clear organic layer had formed, the reaction mixture was poured into hot water and allowed to stand overnight in the hood. The solid that formed was extracted several times with CH_2Cl_2 and the extract was dried over anhydrous Na_2SO_4 . The crude compound that was obtained on evaporation of the extract was purified by column chromatography on silica gel ($\text{CHCl}_3/\text{EtOAc}$).

*9-Butyl-10-para-tolyl-9H-pyreno[4,5-d]imidazole (**4a**)*

Light-yellow solid; 81% yield; M.p. 104–106°C; ^1H NMR (CDCl_3 , 500.13 MHz): δ = 9.07 (dd, J = 7.5 Hz, 1 Hz, 1H), 8.44 (d, J = 8.0 Hz, 1H), 8.16 (d, J = 7.5 Hz, 1H), 8.09–8.13 (m, 3H), 7.99–8.06 (m, 2H), 7.69 (d, J = 8.0 Hz, 2H), 7.39 (d, J = 7.5 Hz, 2H), 4.69 (t, J = 7.5 Hz, 2H), 2.49 (s, 3H), 1.97 (quin, J = 7.5 Hz, 2H), 1.29 (sext, J = 7.5 Hz, 2H), 0.84 ppm (t, J = 7.5 Hz, 3H); ^{13}C NMR (CDCl_3 , 125.77 MHz): δ = 153.1, 139.5, 138.5, 132.4, 131.6, 130.0, 129.5, 128.2, 128.1, 127.6, 126.8, 126.6, 126.3, 125.6, 124.3, 124.1, 123.4, 123.0, 122.7, 119.7, 117.6, 117.6, 46.8, 32.6, 21.5, 19.7, 13.6 ppm; HRMS (ESI): m/z calcd for $C_{28}H_{25}N_2$: 389.2012 [$M+H$]; found: 389.2013.

*10-(Anthracen-9-yl)-9-butyl-9H-pyreno[4,5-d]imidazole (**4b**)*

Yellow solid; 78% yield; M.p. 164–166°C; ^1H NMR (CDCl_3 , 500.13 MHz): δ = 9.13 (d, J = 7.5 Hz, 1H), 8.70 (s, 1H), 8.56 (d, J = 8.0 Hz, 1H), 8.22 (d, J = 8.0 Hz, 2H), 8.07–8.18 (m, 6H), 7.73 (d, J = 8.5 Hz, 2H), 7.53 (t, J = 7.5 Hz, 2H), 7.44 (t, J = 7.5 Hz, 2H), 4.35 (t, J = 8.0 Hz, 2H), 1.83 (quin, J = 7.5 Hz, 2H), 1.08 (sext, J = 7.5 Hz, 2H), 0.54 ppm (t, J = 7.5 Hz, 3H); ^{13}C NMR (CDCl_3 , 125.77 MHz): δ = 149.6, 139.0, 132.6, 132.4, 131.7, 131.4, 129.5, 128.7, 128.2, 127.6, 127.0, 126.8, 126.6, 126.5, 125.9, 125.7, 125.6, 124.53, 124.45, 124.4, 123.5, 123.0, 122.8, 120.0, 117.8, 46.8, 32.4, 19.7, 13.2 ppm; HRMS (ESI): m/z calcd for $C_{35}H_{27}N_2$: 475.2169 [$M+H$]; found: 475.2169.

*9-Butyl-10-(pyren-1-yl)-9H-pyreno[4,5-d]imidazole (**4c**)*

Dark-yellow solid; 84% yield; M.p. 154–156°C; ^1H NMR (CDCl_3 , 500.13 MHz): δ = 9.16 (dd, J = 7.5 Hz, 1 Hz, 1H), 8.57 (d, J = 8.0 Hz, 1H), 8.36 (q, J = 8.0 Hz, 2H), 8.28 (dd, J = 8.0 Hz, 1 Hz, 1H), 8.20–8.24 (m, 5H), 8.13–8.19 (m, 3H), 8.06–8.11 (m, 4H), 4.58 (s, 2H), 1.90 (quin, J = 7.5 Hz, 2H), 1.11 (sext, J = 7.5 Hz, 2H), 0.62 ppm (t, J = 7.5 Hz, 2H); ^{13}C NMR (CDCl_3 , 125.77 MHz): δ = 151.8, 139.0, 132.5, 132.4, 131.7, 131.3, 131.2, 130.9, 128.9, 128.7, 128.6, 128.2, 127.7, 127.4, 126.73, 126.67, 126.5, 126.4, 125.9, 125.8, 125.7, 125.4, 124.8, 124.7, 124.6, 124.52, 124.48, 124.4, 123.6, 123.1, 122.9, 119.9, 117.8, 47.0, 32.4, 19.6, 13.5 ppm; HRMS (ESI): m/z calcd for $C_{37}H_{27}N_2$: 499.2169 [$M+H$]; found: 499.2176.

*4-(9-Butyl-9H-pyreno[4,5-d]imidazol-10-yl)-N,N-diphenylaniline (**4d**)*

Red solid; 72% yield; M.p. 148–150°C; ^1H NMR (CDCl_3 , 500.13 MHz): δ = 9.04 (dd, J = 7.5 Hz, 1 Hz, 1H), 8.43 (d, J = 8.0 Hz, 1H), 8.13 (d, J = 7.5 Hz, 1H), 8.06–8.10 (m, 3H), 7.97–8.03 (m, 2H), 7.64–7.66 (m, 2H), 7.30–7.33 (m, 4H), 7.19–7.24 (m, 6H), 7.09 (t, J = 7.5 Hz, 2H), 4.72 (t, J = 7.5 Hz, 2H), 1.98 (quin, J = 7.5 Hz, 2H), 1.32 (sext, J = 7.5 Hz, 2H), 0.84 ppm (t, J = 7.5 Hz, 3H); ^{13}C NMR (CDCl_3 , 125.77 MHz): δ = 153.0,

149.1, 147.4, 138.6, 132.4, 131.6, 131.0, 129.5, 128.1, 127.6, 126.8, 126.6, 126.3, 125.6, 125.1, 124.8, 124.3, 124.2, 124.1, 123.6, 123.4, 123.0, 122.7, 119.7, 117.6, 46.8, 32.6, 19.6, 13.6 ppm; HRMS (ESI): *m/z* calcd for C₃₉H₃₁N₃Na: 564.2410 [M+Na]; found: 564.2412.

9-Butyl-10-(9-butyl-9H-carbazol-3-yl)-9H-pyreno[4,5-d]imidazole (4e)

Light-yellow solid; 77% yield; M.p. 100–102°C; ¹H NMR (CDCl₃, 500.13 MHz): δ=9.14 (dd, *J*=7.5 Hz, 1.0 Hz, 1H), 8.56 (d, *J*=1.0 Hz, 1H), 8.51 (d, *J*=8.0 Hz, 1H), 8.19 (d, *J*=7.5 Hz, 2H), 8.12–8.15 (m, 3H), 8.02–8.09 (m, 2H), 7.89 (dd, *J*=8.0 Hz, *J*=1.5 Hz, 1H), 7.52–7.58 (m, 2H), 7.48 (d, *J*=8.0 Hz, 1H), 7.31 (t, *J*=7.5 Hz, 1H), 4.81 (t, *J*=7.5 Hz, 2H), 4.37 (t, *J*=7.5 Hz, 2H), 2.03 (quin, *J*=7.5 Hz, 2H), 1.92 (quin, *J*=7.5 Hz, 2H), 1.44 (sext, *J*=7.5 Hz, 2H), 1.30 (sext, *J*=7.5 Hz, 2H), 0.99 (t, *J*=7.5 Hz, 3H), 0.81 ppm (t, *J*=7.5 Hz, 3H); ¹³C NMR (CDCl₃, 125.77 MHz): δ=154.3, 141.0, 138.5, 132.5, 131.7, 128.1, 127.60, 127.57, 126.8, 126.7, 126.3, 126.2, 125.6, 124.3, 124.0, 123.4, 123.14, 123.08, 122.82, 122.77, 122.4, 121.4, 120.7, 119.8, 119.4, 117.6, 109.1, 109.0, 47.0, 43.1, 32.7, 31.2, 20.6, 19.7, 13.9, 13.6 ppm; HRMS (ESI): *m/z* calcd for C₆₇H₆₃N₃Na: 542.2567 [M+Na]; found: 542.2569.

General Procedure for the Synthesis of 10,10'-Aryl-bis(9-(2-ethylhexyl)-9H-pyreno[4,5-d]imidazole) (5a–c)

Pyrene-4,5-dione (0.46 g, 2.0 mmol), the corresponding aldehyde (1.0 mmol), and ammonium acetate (0.62 g, 8 mmol) were dissolved in acetic acid (20 mL) and the resultant mixture was heated at reflux for 24 h. Then, the reaction mixture was cooled and poured into water to obtain a precipitate, which was thoroughly washed with water and dried. The crude product could not be purified because it was not soluble in most organic solvents. Thus, it was suspended in DMF along with K₂CO₃ (0.83 g, 6 mmol) and the resultant mixture was degassed with nitrogen. The mixture was heated at 50°C for 1 h, 2-ethylhexylbromide (0.87 g, 4.5 mmol) was added, and the reaction was continued for a further 48 h. Then, the mixture was poured into water and extracted with CH₂Cl₂. The organic layer was washed several times with brine, dried with Na₂SO₄, and removed under vacuum. The residue was purified by column chromatography on silica gel (CH₂Cl₂/EtOAc).

10,10'-(9,9-Diethyl-9H-fluorene-2,7-diyl)bis(9-(2-ethylhexyl)-9H-pyreno[4,5-d]imidazole) (5a)

Yellow solid; 45% yield; M.p. 126–128°C; ¹H NMR (CDCl₃, 500.13 MHz): δ=9.11 (dd, *J*=7.5 Hz, 1.0 Hz, 2H), 8.57 (d, *J*=8.0 Hz, 2H), 8.20 (t, *J*=7.5 Hz, 4H), 8.06–8.16 (m, 8H), 8.01 (d, *J*=7.5 Hz, 2H), 7.89 (d, *J*=7.5 Hz, 2H), 7.85 (s, 2H), 4.83 (d, *J*=5.5 Hz, 4H), 2.21–2.23 (m, 6H), 1.12 (s, 16H), 0.65–0.76 (m, 12H), 0.47 ppm (t, *J*=5.0 Hz, 6H); ¹³C NMR (CDCl₃, 125.77 MHz): δ=154.4, 150.8, 142.1, 138.9, 132.4, 131.7, 130.4, 129.8, 128.1, 127.7, 127.4, 126.6, 126.5, 125.5, 125.0, 124.5, 124.3, 123.5, 123.2, 122.9, 120.6, 119.9, 118.2, 56.9, 51.4, 38.9, 33.0, 29.9, 28.0, 23.0, 14.0, 10.0, 8.7 ppm; HRMS (ESI): *m/z* calcd for C₆₇H₆₇N₄: 927.5360 [M+H]; found: 927.5356.

4-(9-(2-Ethylhexyl)-9H-pyreno[4,5-d]imidazol-10-yl)-N-(4-(9-(2-ethylhexyl)-9H-pyreno[4,5-d]imidazol-10-yl)phenyl)-N-phenylaniline (5b)

Light-brown solid; 50% yield; M.p. 106–108°C; ¹H NMR (CDCl₃, 500.13 MHz): δ=9.07 (dd, *J*=7.5 Hz, 1.0 Hz, 2H), 8.55 (d, *J*=8.0 Hz, 2H), 8.18 (t, *J*=8.0 Hz, 4H), 8.08–8.14 (m, 6H), 8.06 (t, *J*=7.5 Hz, 2H), 7.76 (d, *J*=8.5 Hz, 4H), 7.36–7.41 (m, 6H), 7.28 (d, *J*=7.5 Hz, 2H), 7.18 (t, *J*=7.5 Hz, 1H), 4.79 (d, *J*=7.0 Hz, 4H), 2.20–2.24 (m, 2H), 1.17 (s, 16H), 0.81–0.84 (m, 6H), 0.70 ppm (s, 6H); ¹³C NMR (CDCl₃, 125.77 MHz): δ=153.9, 148.4, 146.8, 138.6, 132.4, 131.7, 131.4, 129.7, 128.1, 127.6, 127.2, 126.5, 126.4, 125.5, 125.4, 125.3, 124.5, 124.3, 124.2, 123.8, 123.4, 123.2, 122.9, 119.8, 118.1, 50.9, 39.0, 29.7, 27.8, 23.0, 14.0, 9.9 ppm; HRMS (ESI): *m/z* calcd for C₈₈H₈₃N₅Na: 972.4976 [M+Na]; found: 972.4979.

10,10'-(9-Butyl-9H-carbazole-3,6-diyl)bis(9-(2-ethylhexyl)-9H-pyreno[4,5-d]imidazole) (5c)

Light-brown solid; 52% yield; M.p. 122–124°C; ¹H NMR (CDCl₃, 500.13 MHz): δ=9.11 (dd, *J*=7.5 Hz, 1.0 Hz, 2H), 8.65 (t, *J*=7.0 Hz,

2H), 8.58 (d, *J*=8.0 Hz, 2H), 8.05–8.20 (m, 12H), 7.98–8.01 (m, 2H), 7.68 (d, *J*=8.0 Hz, 2H), 4.84–4.91 (m, 4H), 4.50 (t, *J*=7.5 Hz, 2H), 2.19–2.24 (m, 2H), 2.01 (quin, *J*=7.5 Hz, 2H), 1.49 (sext, *J*=7.5 Hz, 2H), 1.01–1.09 (m, 19H), 0.62–0.67 ppm (m, 12H); ¹³C NMR (CDCl₃, 125.77 MHz): δ=154.0, 140.3, 137.8, 131.3, 130.6, 127.3, 126.9, 126.5, 126.0, 125.6, 125.2, 124.3, 123.2, 123.0, 122.3, 122.2, 122.0, 121.9, 121.8, 121.2, 118.7, 117.1, 108.3, 50.2, 42.2, 38.0, 30.0, 28.7, 26.7, 22.0, 21.8, 19.5, 12.9, 12.8, 9.1 ppm; HRMS (ESI): *m/z* calcd for C₆₆H₆₆N₅: 928.5313 [M+H]; found: 928.5309.

Acknowledgements

K.R.J.T. is thankful to the Council of Scientific and Industrial Research, New Delhi (India) for financial support (01(2480)/11/EMR-II). D.K. acknowledges the CSIR for a Research Fellowship.

- [1] a) C. W. Tang, S. A. Vanslyke, *Appl. Phys. Lett.* **1987**, *51*, 913–915; b) C. W. Tang, S. A. Vanslyke, C. H. Chen, *J. Appl. Phys.* **1989**, *65*, 3610–3616; c) Y. R. Sun, N. C. Giebink, H. Kanno, B. W. Ma, M. E. Thompson, S. R. Forrest, *Nature* **2006**, *440*, 908–912; d) S. Reineke, F. Lindner, G. Schwartz, N. Seidler, K. Walzer, B. Lussem, K. Leo, *Nature* **2009**, *459*, 234–238; e) A. C. Grimsdale, K. L. Chan, R. E. Martin, P. G. Jokisz, A. B. Holmes, *Chem. Rev.* **2009**, *109*, 897–1091.
- [2] a) S. Miyaguchi, S. Ishizuka, T. Wakimoto, J. Funaki, Y. Fukuda, H. Kubota, K. Yoshida, T. Watanabe, H. Ochi, T. Sakamoto, M. Tsuchida, I. Ohshita, T. Tohma, *J. Soc. Inf. Disp.* **1999**, *7*, 221–226; b) Z. Y. Xia, J. H. Su, H. H. Fan, K. W. Cheah, H. Tian, C. H. Chen, *J. Phys. Chem. C* **2010**, *114*, 11602–11606; c) Y. J. Chang, T. J. Chow, *J. Mater. Chem.* **2011**, *21*, 3091–3099.
- [3] a) E. Bellmann, S. E. Shaheen, S. Thayumanavan, S. Barlow, R. H. Grubbs, S. R. Marder, B. Kippelen, N. Peyghambarian, *Chem. Mater.* **1998**, *10*, 1668–1676; b) A. P. Kulkarni, C. J. Tonzola, A. Babel, S. A. Jenekhe, *Chem. Mater.* **2004**, *16*, 4556–4573; c) G. Hughes, M. R. Bryce, *J. Mater. Chem.* **2005**, *15*, 94–107; d) Y. Shirota, H. Kageyama, *Chem. Rev.* **2007**, *107*, 953–1010.
- [4] a) H. Tsuji, Y. Yokoi, C. Mitsui, L. Ilies, Y. Sato, E. Nakamura, *Chem. Asian J.* **2009**, *4*, 655–657; b) W. Y. Wong, C. L. Ho, *J. Mater. Chem.* **2009**, *19*, 4457–4482; c) Z. Jiang, T. Ye, C. Yang, D. Yang, M. Zhu, C. Zhong, J. Qin, D. Ma, *Chem. Mater.* **2011**, *23*, 771–777.
- [5] a) V. I. Adamovich, S. R. Cordero, P. I. Djurovich, A. Tamayo, M. E. Thompson, B. W. D'Andrade, S. R. Forrest, *Org. Electron.* **2003**, *4*, 77–87; b) J. A. Hagen, W. Li, A. J. Steckl, J. G. Grote, *Appl. Phys. Lett.* **2006**, *88*, 171109; c) J. W. Kang, D. S. Lee, H. D. Park, Y. S. Park, J. W. Kim, W. I. Jeong, K. M. Yoo, K. Go, S. H. Kim, J. J. Kim, *J. Mater. Chem.* **2007**, *17*, 3714–3719; d) S. O. Jung, J. W. Park, D. M. Kang, J. S. Kim, S. J. Park, P. Kang, H. Y. Oh, J. H. Yang, Y. H. Kim, S. K. Kwon, *J. Nanosci. Nanotechnol.* **2008**, *8*, 4838–4841.
- [6] a) K. Brunner, A. V. Dijken, H. Börner, J. J. A. M. Bastiaansen, N. M. M. Kiggen, B. M. W. Langeveld, *J. Am. Chem. Soc.* **2004**, *126*, 6035–6042; b) P. I. Shih, C. L. Chiang, A. K. Dixit, C. K. Chen, M. C. Yuan, R. Y. Lee, C.-T. Chen, E. W. G. Diau, C. F. Shu, *Org. Lett.* **2006**, *8*, 2799–2802; c) Z. Jiang, Y. Chen, C. Yang, Y. Cao, Y. Tao, J. Qin, D. Ma, *Org. Lett.* **2009**, *11*, 1503–1506.
- [7] a) T. Wakimoto, H. Ochi, S. Kawami, H. Ohata, K. Nagayama, R. Murayama, H. Okuda, T. Tohma, T. Naito, H. Abiko, *J. Soc. Inf. Disp.* **1997**, *5*, 235–240; b) P. E. Burrows, G. Gu, V. Bulovic, Z. Shen, S. R. Forrest, M. E. Thompson, *IEEE Trans. Electron Devices* **1997**, *44*, 1188–1203; c) A. R. Duggal, C. M. Heller, J. J. Shiang, J. Liu, L. N. Lewis, *J. Disp. Technol.* **2007**, *3*, 184–192.
- [8] a) S. W. Wen, M. T. Lee, C. H. Chen, *J. Disp. Technol.* **2005**, *1*, 90–99; b) Z. Q. Gao, Z. H. Li, P. F. Xia, M. S. Wong, K. W. Cheah, C. H. Chen, *Adv. Funct. Mater.* **2007**, *17*, 3194–3199; c) Q. Zhang, J. Li, K. Shizu, S. Huang, S. Hirata, H. Miyazaki, C. Adachi, *J. Am. Chem. Soc.* **2012**, *134*, 14706–14709; d) M. Zhu, T. Ye, C.-G. Li, X. Cao, C. Zhong, D. Ma, J. Qin, C. Yang, *J. Phys. Chem. C* **2011**, *115*, 17965–17972; e) M. Zhu, C. Yang, *Chem. Soc. Rev.* **2013**, *42*, 4963–4976.

- [9] a) K. T. Wong, Y.-M. Chen, Y. T. Lin, H. C. Su, C. C. Wu, *Org. Lett.* **2005**, *7*, 5361–5364; b) K. Wang, F. Zhao, C. Wang, S. Chen, D. Chen, H. Zhang, Y. Liu, D. Ma, Y. Wang, *Adv. Funct. Mater.* **2012**, in press, DOI: 10.1002/adfm.201202981.
- [10] a) K. Müllen, U. Scherf in *Organic Light Emitting Devices: Synthesis Properties and Applications*, Wiley-VCH, Weinheim, **2006**; b) L. S. Hung, C. H. Chen, *Mater. Sci. Eng. R* **2002**, *39*, 143–222.
- [11] a) C. G. Zhen, Y. F. Dai, W. J. Zeng, Z. Ma, Z. K. Chen, J. Kieffer, *Adv. Funct. Mater.* **2011**, *21*, 699–707; b) T. Zhang, D. Liu, Q. Wang, R. Wang, H. Ren, J. Li, *J. Mater. Chem.* **2011**, *21*, 12969–12976; c) C. Liu, Y. Li, Y. Zhang, C. Yang, H. Wu, J. Qin, Y. Cao, *Chem. Eur. J.* **2012**, *18*, 6928–6934; d) Z. Jiang, Z. Liu, C. Yang, C. Zhong, J. Qin, G. Yu, Y. Liu, *Adv. Funct. Mater.* **2009**, *19*, 3987–3995; e) C. Liu, Y. Gu, Q. Fu, N. Sun, C. Zhong, D. Ma, J. Qin, C. Yang, *Chem. Eur. J.* **2012**, *18*, 13828–13835.
- [12] a) M. Zhu, Q. Wang, Y. Gu, X. Cao, C. Zhong, D. Ma, J. Qin, C. Yang, *J. Mater. Chem.* **2011**, *21*, 6409–6415; b) I. Cho, S. H. Kim, J. H. Kim, S. Park, S. Y. Park, *J. Mater. Chem.* **2012**, *22*, 123–129; c) H. Park, J. Lee, I. Kang, H. Y. Chu, J. I. Lee, S. K. Kwon, Y. H. Kim, *J. Mater. Chem.* **2012**, *22*, 2695–2700.
- [13] a) X. Feng, J. Y. Hu, L. Yi, N. Seto, Z. Tao, C. Redshaw, M. R. J. Elsegood, T. Yamato, *Chem. Asian J.* **2012**, *7*, 2854–2863; b) B. R. Kaafarani, A. O. El-Ballouli, R. Trattning, A. Fonari, S. Sax, B. Wex, C. Risko, R. S. Khnayzer, S. Barlow, D. Patra, T. V. Timofeeva, E. J. W. List, J. E. Brédas, S. R. Marder, *J. Mater. Chem. C* **2013**, *1*, 1638–1650; c) D. Kumar, K. R. J. Thomas, Y. L. Chen, Y. C. Jou, J. H. Jou, *Tetrahedron* **2013**, *69*, 2594–2602.
- [14] a) P. C. Bevilacqua, R. Kierzek, K. A. Johnson, D. H. Turner, *Science* **1992**, *258*, 1355–1358; b) N. Karl in *Organic Electronic Materials, Part II: Low Molecular Weight Organic Solids*, Vol. 41 (Eds.: R. Farchioni, G. Gross), Springer, Berlin, **2001**, pp. 283–326; c) N. Karl, *Synth. Met.* **2003**, *133–134*, 649–657; d) C. Tang, F. Liu, Y. J. Xia, L. H. Xie, A. Wei, S. B. Li, Q. L. Fan, W. Huang, *J. Mater. Chem.* **2006**, *16*, 4074–4080.
- [15] a) J. Y. Hu, T. Yamato in *Organic Light Emitting Diodes-Material, Process and Devices* (Ed.: S. H. Ko), InTech, Rijeka, Croatia, **2011**, pp. 21–60; b) T. M. Figueira-Duarte, K. Müllen, *Chem. Rev.* **2011**, *111*, 7260–7314; c) K. R. J. Thomas, N. Kapoor, M. N. K. P. Bolisetty, J. H. Jou, Y. L. Chen, Y. C. Jou, *J. Org. Chem.* **2012**, *77*, 3921–3932.
- [16] a) T. Oyamada, H. Uchiuzou, S. Akiyama, Y. Oku, N. Shimoji, K. Matsushige, H. Sasabe, C. Adachi, *J. Appl. Phys.* **2005**, *98*, 074506; b) Y. Wang, H. Wang, Y. Liu, C. Di, Y. Sun, W. Wu, G. Yu, D. Zhang, D. Zhu, *J. Am. Chem. Soc.* **2006**, *128*, 13058–13059; c) F. Moggia, C. Videlot-Ackermann, J. Ackermann, P. Raynal, H. Brisset, F. Fages, *J. Mater. Chem.* **2006**, *16*, 2380–2386; d) S. Z. Bisri, T. Takahashi, T. Takenobu, M. Yahiro, C. Adachi, Y. Iwasa, *Jpn. J. Appl. Phys.* **2007**, *46*, L596–L598; e) M. Ashizawa, K. Yamada, A. Fukaya, R. Kato, K. Hara, J. Takeya, *Chem. Mater.* **2008**, *20*, 4883–4890; f) L. Zöphel, D. Beckmann, V. Enkelmann, D. Chercak, R. Rieger, K. Müllen, *Chem. Commun.* **2011**, *47*, 6960–6962.
- [17] G. D. Sharma, P. Suresh, J. A. Mikroyannidis, M. M. Stylianakis, *J. Mater. Chem.* **2010**, *20*, 561–567.
- [18] a) Y. Oseki, M. Fujitsuka, M. Sakamoto, T. Majima, *J. Phys. Chem. A* **2007**, *111*, 9781–9788; b) A. Baheti, C. P. Lee, K. R. J. Thomas, K. C. Ho, *Phys. Chem. Chem. Phys.* **2011**, *13*, 17210–17221; c) K. R. J. Thomas, N. Kapoor, C. P. Lee, K. C. Ho, *Chem. Asian J.* **2012**, *7*, 738–750; d) C. C. Yu, K. J. Jiang, J. H. Huang, F. Zhang, X. Bao, F. W. Wang, L. M. Yang, Y. Song, *Org. Electron.* **2013**, *14*, 445–450.
- [19] a) L. Altschuler, E. Berliner, *J. Am. Chem. Soc.* **1966**, *88*, 5837–5845; b) A. Miyazawa, A. Tsuge, T. Yamato, M. Tashiro, *J. Org. Chem.* **1991**, *56*, 4312–4314; c) Z. Liu, Y. Wang, Y. Chen, J. Liu, Q. Fang, C. Kleberg, T. B. Marder, *J. Org. Chem.* **2012**, *77*, 7124–7128.
- [20] F. Liu, C. Tang, Q. Q. Chen, F. F. Shi, H. B. Wu, L. H. Xie, B. Peng, W. Wei, Y. Cao, W. Huang, *J. Phys. Chem. C* **2009**, *113*, 4641–4647.
- [21] a) J. N. Moorthy, P. Natarajan, P. Venkatakrishnan, D. F. Huang, T. J. Chow, *Org. Lett.* **2007**, *9*, 5215–5218; b) K. R. Wee, H. C. Ahn, H. J. Son, W. S. Han, J. E. Kim, D. W. Cho, S. O. Kang, *J. Org. Chem.* **2009**, *74*, 8472–8475; c) J. Y. Hu, M. Era, M. R. J. Elsegood, T. Yamato, *Eur. J. Org. Chem.* **2010**, 72–79; d) T. M. Figueira-Duarte, P. G. D. Rosso, R. Trattning, S. Sax, E. J. W. List, K. Müllen, *Adv. Mater.* **2010**, *22*, 990–993.
- [22] R. Trattning, T. M. F. Duarte, D. Lorbach, W. Wiedemair, S. Sax, S. Winkler, A. Vollmer, N. Koch, M. Manca, M. A. Loi, M. Baumgarten, E. J. W. List, K. Müllen, *Opt. Express* **2011**, *19*, A1281–A1292.
- [23] K. C. Wu, P. J. Ku, C. S. Lin, H. T. Shih, F. I. Wu, M. J. Huang, J. J. Lin, I. C. Chen, C. H. Cheng, *Adv. Funct. Mater.* **2008**, *18*, 67–75.
- [24] a) Z. Zhao, X. Xu, Z. Jiang, P. Lu, G. Yu, Y. Liu, *J. Org. Chem.* **2007**, *72*, 8345–8353; b) Z. Zhao, X. Xu, H. Wang, P. Lu, G. Yu, Y. Liu, *J. Org. Chem.* **2008**, *73*, 594–602.
- [25] K. L. Chan, J. P. F. Lim, X. Yang, A. Dodabalapur, G. E. Jabbour, A. Sellinger, *Chem. Commun.* **2012**, *48*, 5106–5108.
- [26] a) W. Sotoyama, H. Sato, M. Kinoshita, T. Takahashi, A. Matsuura, J. Kodama, N. Sawatari, H. Inoue, *SID Digest* **2003**, *45*, 1294–1295; b) P. Sonar, M. S. Soh, Y. H. Cheng, J. T. Henssler, A. Sellinger, *Org. Lett.* **2010**, *12*, 3292–3295; c) Z. Wang, C. Xu, W. Wang, X. Dong, B. Zhao, B. Ji, *Dyes Pigm.* **2012**, *92*, 732–736.
- [27] a) Y. Xing, X. Xu, P. Zhang, W. Tian, G. Yu, P. Lu, Y. Liu, D. Zhu, *Chem. Phys. Lett.* **2005**, *408*, 169–173; b) T. Kumchoo, V. Promarak, T. Sudyoardsuk, M. Sukwattanasinitt, P. Rashatasakhon, *Chem. Asian J.* **2010**, *5*, 2162–2167.
- [28] a) S. L. Tao, Z. K. Peng, X. H. Zhang, P. F. Wang, C. S. Lee, S. T. Lee, *Adv. Funct. Mater.* **2005**, *15*, 1716–1721; b) C. Tang, F. Liu, Y. J. Xia, J. Lin, L. H. Xie, G. Y. Zhong, Q. L. Fan, W. Huang, *Org. Electron.* **2006**, *7*, 155–162; c) Z. Peng, S. Tao, X. Zhang, *J. Phys. Chem. C* **2008**, *112*, 2165–2169; d) F. Liu, L. H. Xie, C. Tang, J. Liang, Q. Q. Chen, B. Peng, W. Wei, Y. Cao, W. Huang, *Org. Lett.* **2009**, *11*, 3850–3853; e) Z. Wang, C. Xu, W. Wang, W. Fu, L. Niu, B. Ji, *Solid-State Electron.* **2010**, *54*, 524–526; f) S. Tao, Y. Zhou, C. S. Lee, X. Zhang, S. T. Lee, *Chem. Mater.* **2010**, *22*, 2138–2141; g) A. Thangthong, N. Prachumrak, R. Tarsang, T. Keawin, S. Jungsuttiwong, T. Sudyoardsuk, V. Promarak, *J. Mater. Chem.* **2012**, *22*, 6869–6877.
- [29] a) W. L. Jia, T. M. Cormick, Q. D. Liu, H. Fukutani, M. Motala, R. Y. Wang, Y. Tao, S. Wang, *J. Mater. Chem.* **2004**, *14*, 3344–3350; b) K. R. J. Thomas, M. Velusamy, J. T. Lin, C. H. Chuen, Y. T. Tao, *J. Mater. Chem.* **2005**, *15*, 4453–4459; c) S. L. Lai, Q. X. Tong, M. Y. Chan, T. W. Ng, M. F. Lo, S. T. Lee, C. S. Lee, *J. Mater. Chem.* **2011**, *21*, 1206–1211.
- [30] S. Tao, Y. Zhou, C. S. Lee, S. T. Lee, D. Huang, X. Zhang, *J. Phys. Chem. C* **2008**, *112*, 14603–14606.
- [31] a) Y. L. Liao, C. Y. Lin, K. T. Wong, T. H. Hou, W. Y. Hung, *Org. Lett.* **2007**, *9*, 4511–4514; b) M. Y. Lai, C. H. Chen, W. S. Huang, J. T. Lin, T. H. Ke, L. Y. Chen, M. H. Tsai, C. C. Wu, *Angew. Chem.* **2008**, *120*, 591–595; *Angew. Chem. Int. Ed.* **2008**, *47*, 581–585; c) C. H. Chen, W. S. Huang, M. Y. Lai, W. C. Tsao, J. T. Lin, Y. H. Wu, T. H. Ke, L. Y. Chen, C. C. Wu, *Adv. Funct. Mater.* **2009**, *19*, 2661–2670; d) Y. M. Chen, W. Y. Hung, H. W. You, A. Chaskar, H. C. Ting, H. F. Chen, K. T. Wong, Y. H. Liu, *J. Mater. Chem.* **2011**, *21*, 14971–14978; e) D. Thirion, J. Rault-Berthelot, L. Vignau, C. Poriel, *Org. Lett.* **2011**, *13*, 4418–4421.
- [32] a) R. Y. Wang, W. L. Jia, H. Aziz, G. Vamvounis, S. Wang, N. X. Hu, Z. D. Popović, J. A. Coggan, *Adv. Funct. Mater.* **2005**, *15*, 1483–1487; b) J. F. Lee, Y. C. Chen, J. T. Lin, C. C. Wu, C. Y. Chen, C. A. Dai, C. Y. Chao, H. L. Chen, W. B. Liau, *Tetrahedron* **2011**, *67*, 1696–1702.
- [33] a) C. J. Kuo, T. Y. Li, C. C. Lien, C. H. Liu, F.-I. Wu, M. J. Huang, *J. Mater. Chem.* **2009**, *19*, 1865–1871; b) Z. Wang, P. Lu, S. Chen, Z. Gao, F. Shen, W. Zhang, Y. Xu, H. S. Kwok, Y. Ma, *J. Mater. Chem.* **2011**, *21*, 5451–5456; c) Y. Zhang, S. L. Lai, Q. X. Tong, M. Y. Chan, T. W. Ng, Z. C. Wen, G. Q. Zhang, S. T. Lee, H. L. Kwong, C. S. Lee, *J. Mater. Chem.* **2011**, *21*, 8206–8214; d) Y. Zhang, S. L. Lai, Q. X. Tong, M. F. Lo, T. W. Ng, M. Y. Chan, Z. C. Wen, J. He, K. S. Jeff, X. L. Tang, W. M. Liu, C. C. Ko, P. F. Wang, C. S. Lee, *Chem. Mater.* **2012**, *24*, 61–70.
- [34] a) J. G. Guo, Y. M. Cui, H. X. Lin, X. Z. Xie, H. F. Chen, *J. Photochem. Photobiol. A* **2011**, *219*, 42–49; b) H. F. Chen, Y. M. Cui, J. G. Guo, H. X. Lin, *Dyes Pigm.* **2012**, *94*, 583–591.

- [35] a) Y. Li, M. K. Fung, Z. Xie, S. T. Lee, L. S. Hung, J. Shi, *Adv. Mater.* **2002**, *14*, 1317–1321; b) Z. Ge, T. Hayakawa, S. Ando, M. Ueda, T. Akiike, H. Miyamoto, T. Kajita, M. Kakimoto, *Chem. Mater.* **2008**, *20*, 2532–2537; c) J. Huang, J. H. Su, X. Li, M. K. Lam, K. M. Fung, H. H. Fan, K. W. Cheah, C. H. Chen, H. Tian, *J. Mater. Chem.* **2011**, *21*, 2957–2964.
- [36] a) G. M. Badger in *Aromatic Character and Aromaticity*, Cambridge University Press, London, **1969**; b) R. G. Harvey, in *Polycyclic Aromatic Hydrocarbons*, Wiley, New York, **1997**; c) R. W. A. Havenith, J. H. V. Lenthe, F. Dijkstra, L. W. Jenneskens, *J. Phys. Chem. A* **2001**, *105*, 3838–3845.
- [37] D. Kumar, K. R. J. Thomas, C. P. Lee, K. C. Ho, *Org. Lett.* **2011**, *13*, 2622–2625.
- [38] J. Hu, D. Zhang, F. W. Harris, *J. Org. Chem.* **2005**, *70*, 707–708.
- [39] D. Kumar, K. R. J. Thomas, *J. Photochem. Photobiol. A* **2011**, *218*, 162–173.
- [40] a) K. Kalyanasundaram, J. K. Thomas, *J. Am. Chem. Soc.* **1977**, *99*, 2039–2044; b) D. C. Dong, M. A. Winnik, *Photochem. Photobiol.* **1982**, *35*, 17–21; c) D. S. Karpovich, G. J. Blanchard, *J. Phys. Chem.* **1995**, *99*, 3951–3958.
- [41] a) B. Valeur in *Molecular Fluorescence: Principles and Applications*, Wiley-VCH, Weinheim, **2002**, pp. 211–213; b) M. Jozefowicz, J. R. Heldt, *Spectrochim. Acta Part A* **2007**, *67*, 316–320; c) G. V. Loukova, A. A. Milov, V. P. Vasiliev, V. A. Smirnov, *Russ. Chem. Bull. Int. Ed.* **2008**, *57*, 1166–1171.
- [42] C. Reichardt, *Chem. Rev.* **1994**, *94*, 2319–2358.
- [43] a) S. K. Dogra, *J. Photochem. Photobiol. A* **2005**, *172*, 185–195; b) X. Sun, Y. Liu, X. Xu, C. Yang, G. Yu, S. Chen, Z. Zhao, W. Qiu, Y. Li, D. Zhu, *J. Phys. Chem. B* **2005**, *109*, 10786–10792.
- [44] a) H. Detert, V. Schmitt, *J. Phys. Org. Chem.* **2006**, *19*, 603–607; b) H. H. Hammud, K. H. Bouhadir, M. S. Masoud, A. M. Ghanouni, S. A. Assi, *J. Solution Chem.* **2008**, *37*, 895–917.
- [45] a) S. A. Tucker, L. E. Cretella, R. Waris, K. W. Street, Jr., W. E. Acree, Jr., J. C. Fetzer, *Appl. Spectrosc.* **1990**, *44*, 269–273; b) S. A. Tucker, W. E. Acree, Jr., M. J. Tanga, *Appl. Spectrosc.* **1991**, *45*, 911–915.
- [46] N. J. Turro, V. Ramamurthy, J. C. Scaiano in *Principles of Molecular Photochemistry: An Introduction*, University Science Books, Sausalito, **2009**.
- [47] a) J. N. Demas, G. A. Crosby, *J. Phys. Chem.* **1971**, *75*, 991–1024; b) G. Jones II., W. R. Jackson, C. Y. Choi, W. R. Bergmark, *J. Phys. Chem.* **1985**, *89*, 294–300.
- [48] a) E. J. Bowen, F. Wokes in *Fluorescence of Solutions*, Longmans, Green and Co., London, **1953**; b) B. L. Van Duuren, *Chem. Rev.* **1963**, *63*, 325–354.
- [49] X. Wu, A. P. Davis, P. C. Lambert, L. K. Steffen, O. Toy, A. J. Fry, *Tetrahedron* **2009**, *65*, 2408–2414.
- [50] J. Pommerehne, H. Vestweber, W. Guss, R. F. Mahrt, H. Bässler, M. Porsch, J. Daub, *Adv. Mater.* **1995**, *7*, 551–554.
- [51] a) X. Zhang, Q. Li, J. B. Ingels, A. C. Simmonett, S. E. Wheeler, Y. Xie, R. B. King, H. F. Schaefer III., F. A. Cotton, *Chem. Commun.* **2006**, 758–760; b) Y. H. Chen, S. L. Lin, Y. C. Chang, Y. C. Chen, J. T. Lin, R. H. Lee, W. J. Kuo, R. J. Jeng, *Org. Electron.* **2012**, *13*, 43–52.
- [52] a) Y. Kuwabara, H. Ogawa, H. Inada, N. Noma, Y. Shirota, *Adv. Mater.* **1994**, *6*, 677–679; b) V. Promarak, M. Ichikawa, T. Sudyoad-suk, S. Saengsuwan, S. Jungsuttiwong, T. Keawin, *Synth. Met.* **2007**, *157*, 17–22; c) C. W. Kim, M. C. Choi, J. C. Hwang, C. S. Ha, *J. Nanosci. Nanotechnol.* **2012**, *12*, 4219–4223; d) Z. Zhao, C. Y. K. Chan, S. Chen, C. Deng, J. W. Y. Lam, C. K. W. Jim, Y. Hong, P. Lu, Z. Chang, X. Chen, P. Lu, H. S. Kwok, H. Qiu, B. Z. Tang, *J. Mater. Chem.* **2012**, *22*, 4527–4534.
- [53] Gaussian 09, Revision A.02, M. J. Frisch, G. W. Trucks, H. B. Schlegel, G. E. Scuseria, M. A. Robb, J. R. Cheeseman, G. Scalmani, V. Barone, B. Mennucci, G. A. Petersson, H. Nakatsuji, M. Caricato, X. Li, H. P. Hratchian, A. F. Izmaylov, J. Bloino, G. Zheng, J. L. Sonnenberg, M. Hada, M. Ehara, K. Toyota, R. Fukuda, J. Hasegawa, M. Ishida, T. Nakajima, Y. Honda, O. Kitao, H. Nakai, T. Vreven, J. A., Jr., Montgomery, J. E. Peralta, F. Ogliaro, M. Bearpark, J. J. Heyd, E. Brothers, K. N. Kudin, V. N. Staroverov, R. Kobayashi, J. Normand, K. Raghavachari, A. Rendell, J. C. Burant, S. S. Iyengar, J. Tomasi, M. Cossi, N. Rega, N. J. Millam, M. Klene, J. E. Knox, J. B. Cross, V. Bakken, C. Adamo, J. Jaramillo, R. Gomperts, R. E. Stratmann, O. Yazyev, A. J. Austin, R. Cammi, C. Pomelli, J. W. Ochterski, R. L. Martin, K. Morokuma, V. G. Zakrzewski, G. A. Voth, P. Salvador, J. J. Dannenberg, S. Dapprich, A. D. Daniels, Ö. Farkas, J. B. Foresman, J. V. Ortiz, J. Ciosowski, D. J. Fox, Gaussian, Inc., Wallingford, CT, **2009**.
- [54] A. D. Becke, *J. Chem. Phys.* **1993**, *98*, 1372–1377.
- [55] C. Lee, W. Yang, R. G. Parr, *Phys. Rev. B* **1988**, *37*, 785–789.
- [56] G. Lai, X. R. Bu, J. Santos, E. A. Mintz, *Synlett* **1997**, *11*, 1275–1276.
- [57] Y. Song, C. A. Di, Z. Wei, T. Zhao, W. Xu, Y. Liu, D. Zhang, D. Zhu, *Chem. Eur. J.* **2008**, *14*, 4731–4740.

Received: February 28, 2013

Revised: April 16, 2013

Published online: ■■■, 0000